Clinical Cancer Research

Combined Inhibition of STAT3 and DNA Repair in Palbociclib-Resistant ER-Positive Breast Cancer

Nicole M. Kettner[1], Smruthi Vijayaraghavan[1], Merih Guray Durak[1], Tuyen Bui[1], Mehrnoosh Kohansal[1], Min Jin Ha[2], Bin Liu[3], Xiayu Rao[4], Jing Wang[4], Min Yi[5], Jason P.W. Carey[1], Xian Chen[1], T. Kris Eckols[6], Akshara S. Raghavendra[7], Nuhad K. Ibrahim[7], Meghan Sri Karuturi[7], Stephanie S. Watowich[8], Aysegul Sahin[9], David J. Tweardy[6,10], Kelly K. Hunt[5], Debu Tripathy[7], and Khandan Keyomarsi[1]

Abstract

Purpose: Cyclin-dependent kinase 4/6 (CDK4/6) inhibitors are currently used in combination with endocrine therapy to treat advanced hormone receptor–positive, HER2-negative breast cancer. Although this treatment doubles time to progression compared with endocrine therapy alone, about 25%–35% of patients do not respond, and almost all patients eventually acquire resistance. Discerning the mechanisms of resistance to CDK4/6 inhibition is crucial in devising alternative treatment strategies.

Experimental Design: Palbociclib-resistant cells (MCF-7 and T47D) were generated in a step-wise dose-escalading fashion. Whole-exome sequencing, genome-wide expression analysis, and proteomic analysis were performed in both resistant and parental (sensitive) cells. Pathway alteration was assessed mechanistically and pharmacologically. Biomarkers of altered pathways were examined in tumor samples from patients with palbociclib-treated breast cancer whose disease progressed while on treatment.

Results: Palbociclib-resistant cells are cross-resistant to other CDK4/6 inhibitors and are also resistant to endocrine therapy (estrogen receptor downregulation). IL6/STAT3 pathway is induced, whereas DNA repair and estrogen receptor pathways are downregulated in the resistant cells. Combined inhibition of STAT3 and PARP significantly increased cell death in the resistant cells. Matched tumor samples from patients with breast cancer who progressed on palbociclib were examined for deregulation of estrogen receptor, DNA repair, and IL6/STAT3 signaling, and results revealed that these pathways are all altered as compared with the pretreatment tumor samples.

Conclusions: Palbociclib resistance induces endocrine resistance, estrogen receptor downregulation, and alteration of IL6/STAT3 and DNA damage response pathways in cell lines and patient samples. Targeting IL6/STAT3 activity and DNA repair deficiency using a specific STAT3 inhibitor combined with a PARP inhibitor could effectively treat acquired resistance to palbociclib.

Introduction

Breast cancer is highly heterogeneous and can be classified on the basis of histopathology, grade, stage, hormone receptor status, and genomic landscape. Prognosis and treatment strategies are guided by determination of hormone receptor status, such as estrogen receptor (ER) and HER2 receptor status, which are key mediators of cell growth pathways that can be targeted pharmacologically. ER-positive/HER2-negative breast cancer represents the largest subtype of breast cancer. For decades, the treatment focus has been on endocrine therapy. However, patients receiving endocrine therapy for early-stage ER-positive breast cancer only have a partial reduction in their risk of recurrence and mortality, and those with advanced disease either progress shortly after initiating therapy (intrinsic resistance), or ultimately experience progression after initial response or stability (acquired resistance; ref. 1). Recent advancements in biologically targeted therapies

[1]Department of Experimental Radiation Oncology, The University of Texas MD Anderson Cancer Center, Houston, Texas. [2]Department of Biostatistics, The University of Texas MD Anderson Cancer Center, Houston, Texas. [3]Department of Human Genetics, The University of Texas MD Anderson Cancer Center, Houston, Texas. [4]Department of Bioinformatics and Computational Biology, The University of Texas MD Anderson Cancer Center, Houston, Texas. [5]Department of Breast Surgical Oncology, The University of Texas MD Anderson Cancer Center, Houston, Texas. [6]Department of Infectious Diseases, Infection Control & Employee Health, Division of Internal Medicine, The University of Texas MD Anderson Cancer Center, Houston, Texas. [7]Department of Breast Medical Oncology, The University of Texas MD Anderson Cancer Center, Houston, Texas. [8]Department of Immunology, The University of Texas MD Anderson Cancer Center, Houston, Texas. [9]Department of Pathology, The University of Texas MD Anderson Cancer Center, Houston, Texas. [10]Department of Molecular & Cellular Oncology, The University of Texas MD Anderson Cancer Center, Houston, Texas.

Note: Supplementary data for this article are available at Clinical Cancer Research Online (http://clincancerres.aacrjournals.org/).

S. Vijayaraghavan and M.G. Durak contributed equally to this article.

Current address for S. Vijayaraghavan: Janssen R&D, Spring House, Pennsylvania; and current address for M.G. Durak, Dokuz Eylul University Faculty of Medicine, Inciralti-Izmir, Turkey.

Corresponding Authors: Khandan Keyomarsi, The University of Texas MD Anderson Cancer Center, 6565 MD Anderson Boulevard, Unit 1052, Houston, TX 77030. Phone: 713-792-4845; Fax: 713-794-5369; E-mail: kkeyomar@mdanderson.org; and Nicole M. Kettner, E-mail: NMKettner@mdanderson.org

Clin Cancer Res 2019;25:3996–4013

doi: 10.1158/1078-0432.CCR-18-3274

Translational Relevance

The majority of breast cancer–related deaths are due to progression of metastatic estrogen receptor (ER)–positive disease. Identification of targetable biomarkers to predict treatment strategies to circumvent resistance to cyclin-dependent kinase 4/6 (CDK4/6) class of inhibitors, which are currently used in combination with endocrine therapy in patients with ER-positive metastatic breast cancer, will be instrumental in improving survival. We show that ER-positive breast cancer cells acquire resistance to palbociclib (CDK4/6 inhibitor) by downregulation of ER protein and DNA repair machinery and upregulation of the IL6/STAT3 pathway, which is overcome by treatment with STAT3 and PARP inhibitors. Matched biopsies from patients with breast cancer who progressed on palbociclib showed deregulation in DNA repair, ER, and IL6/STAT3 as compared with their pretreatment biopsy samples. By identifying and validating these mediators (or drivers) of palbociclib resistance, we propose that patients who progress on palbociclib can be targeted using clinically available inhibitors to STAT3 and DNA repair to circumvent resistance and improve clinical outcomes.

against mTOR, PI3K, and cyclin-dependent kinase 4/6 (CDK4/6), have proven successful in delaying progression when added to endocrine therapy, yet no improvement in long-term survival has been observed to date (2).

Three CDK4/6 inhibitors, palbociclib, ribociclib, and abemaciclib, are used in the first- or second-line settings in combination with either aromatase inhibitors or the ER downregulator, fulvestrant on the basis of increased progression-free survival as compared with endocrine therapy alone (2, 3). Despite these promising clinical advances, it is expected that the majority of patients will develop resistance following long-term (median of about 24 months in first-line and 12 months in second-line) treatment. For patients experiencing resistance to CDK4/6 inhibitors, novel combination treatment strategies are needed to delay progression or to improve survival.

Previous studies have shown resistance to palbociclib or abemaciclib arises from bypass or deregulation of the G_1–S checkpoint, and this occurs either through amplification of *CDK6* or cyclin E (*CCNE1*) or loss of the retinoblastoma (*Rb1*; refs. 4, 5). Recent analysis evaluating circulating tumor DNA from patients who received fulvestrant or fulvestrant + palbociclib (PALOMA-3) revealed clonal evolution involving *ESR1*, *PIK3CA*, and *Rb1* loss (6). *ESR1* and *PIK3CA* aberrations occurred in both treatment cohorts but *Rb1* only occurred in the palbociclib-treated cohort. Other studies aimed at evaluating additional mechanisms of resistance through phosphoproteome analysis have revealed enhanced MAPK signaling in palbociclib-resistant prostate cancer (7) and activation of the AKT pathway in ER-positive breast cancer (8). On the basis of these specific protein alterations, therapeutic strategies to prevent or circumvent CDK4/6 inhibitor resistance by either MEK inhibition (7) or PI3K inhibition (8) have been proposed.

In light of emerging research on mechanisms of acquired resistance to CDK4/6 inhibition, translational studies are needed to identify clinically available drugs that effectively target resistant tumors, as well as biomarkers that can identify resistant tumors. While *Rb1* loss and *CCNE1* amplification (known mechanisms of G_1–S deregulation) are the currently predicted mechanisms of acquired resistance, it is possible that resistant cells have alterations not directly related to cell cycle. Here, we have uncovered novel mechanisms (i.e., alteration in DNA repair and IL6/STAT3 pathways), by which the ER-positive breast cancer cells acquire resistance to palbociclib and, through detailed omics approaches and validation studies, identified treatment options that effectively target such resistance. Using matched pre- and postprogression tumor samples from patients with breast cancer who progressed while on palbociclib, we found that the pathways that were identified in resistant cell lines (ER, DNA repair, and IL6/STAT3) were also altered in patients with acquired or intrinsic resistance to palbociclib. Collectively these results suggest that targeting IL6/STAT3 and DNA repair deficiency in combination can effectively treat acquired resistance to palbociclib.

Materials and Methods

Cell lines and culture conditions

MCF-7 and T47D cell lines used in this study were obtained from ATCC. Palbociclib-resistant cell lines were generated by culturing cells in media supplemented with palbociclib at increasing concentrations for 6 months starting at 1 μmol/L and reaching a final dose of 5 μmol/L. Resistant cells were maintained in media supplemented with 5 μmol/L palbociclib. All experiments were conducted in the absence of palbociclib-supplemented media unless otherwise noted. Palbociclib was obtained from Pfizer, Inc and was diluted in DMSO for *in vitro* use. For gamma irradiation studies, cells were subjected to 0–6 Gy using XRAD 320 X-Ray irradiator. Cells were maintained in culture for 1 week prior to imaging and cell viability analysis. All cells were free of *Mycoplasma* contamination and were authenticated regularly (every 6 months) by karyotype and short tandem repeat analysis at The University of Texas MD Anderson Cancer Center (MDACC) Characterized Cell Line Core Facility (Houston, TX). Detailed procedures for all *in vitro* assays [high-throughput dose–response survival, cell proliferation, flow cytometry, Western blot, qRT-PCR, immunofluorescence (IF), migration assays, mammosphere formation assays, mammary acini morphogenesis assays, shRNA/siRNA knockdown, kinase assays, and reverse phase protein array (RPPA) analysis] were described previously (9–12) and are also included in the Supplementary Materials and Methods.

IL6 ELISA and recombinant IL6 treatment

The Quantikine Human IL6 ELISA Kit (R&D Systems) was used to measure IL6 in cell culture supernatants following the manufacturer's protocol. Human recombinant IL6 and soluble IL6 receptor α from PeproTech were added to the media every 3 days and cultured for 6 days.

Whole-exome sequencing, RNA sequencing, and gene set enrichment analysis

DNA was extracted from cell lysates using QIAamp DNA Mini Kit (Qiagen) and total RNA was isolated from cell cultures using an RNeasy Kit with DNase treatment according to the manufacturer's protocol (Qiagen). Isolated DNA was submitted to Admera Health for whole-exome sequencing (WES) using the Illumina platform and RNA samples were submitted to the Sequencing and

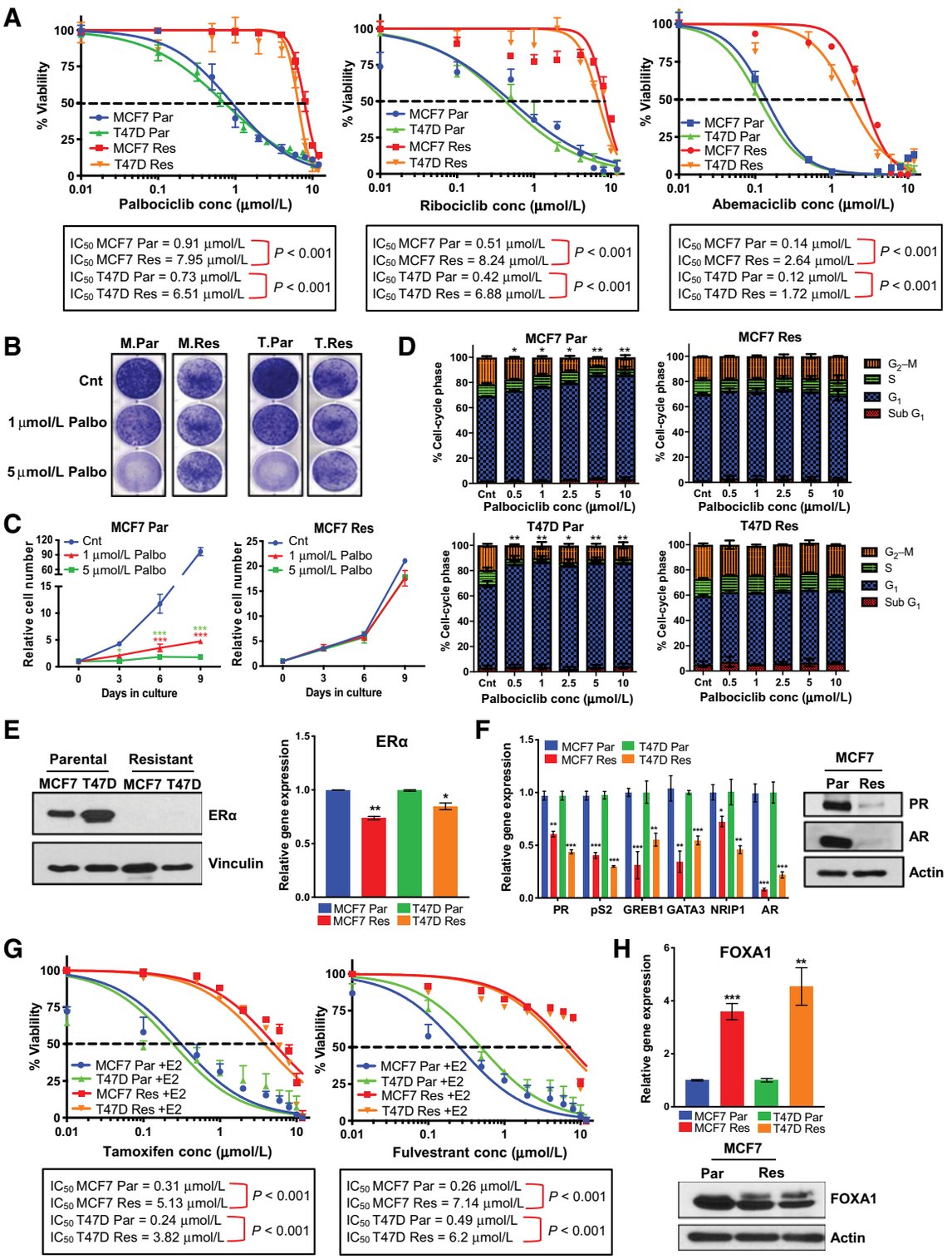

Figure 1.

Palbociclib-resistant cells are cross-resistant to other approved CDK4/6 inhibitors and are intrinsically resistant to endocrine therapy. **A,** Dose–response curves in MCF-7 and T47D parental (Par) and resistant (Res) cells depicting the effect of treatment with varying concentrations (conc) of palbociclib, ribociclib, or abemaciclib (0.01–12 μmol/L) for 6 days and recovery for 6 days. Dashed line depicts IC_{50} values. **B,** Clonogenic assay showing effect of 1 and 5 μmol/L palbociclib (Palbo) treatment on the proliferation of MCF-7 (M) and T47D (T) parental (Par) and resistant (Res) cell lines. (*Continued on the following page.*)

Microarray Facility at MDACC. Detailed procedures are described in Supplementary Materials and Methods. RNA-sequencing (RNA-seq) data have been deposited in the NCBI Gene Expression Omnibus with accession code GSE128056. WES data have been deposited in the NCBI Sequence Read Archive with NCBI BioProject accession code PRJNA526223.

Experimental metastasis assay

Cells (1×10^6) were injected into the tail vein of 4- to 6-weeks old female immunodeficient mice (nude). After 10 weeks, lungs were isolated, fixed, and stained with standard hematoxylin and eosin (H&E). All animal studies were approved by the MD Anderson Institutional Animal Care and Use Committee.

Patient population

A prospectively maintained database at MDACC was used to identify patients who received palbociclib in combination with endocrine therapy for metastatic ER-positive, HER2-negative breast cancer between February 2015 and July 2018. Data elements collected included: patient demographics including date of birth, race, menopausal status, gender, and date of diagnosis of primary breast cancer, tumor characteristics including clinical stage at presentation, ER, progesterone receptor (PR), and HER2 status using 2010 and 2013 American Society of Clinical Oncology (ASCO)/College of American Pathologists (CAP) guidelines, and tumor grade. The MDACC Institutional Review Board approved the study.

IHC of patient samples

IHC was performed on FFPE tissue sections for ER, PR, and pY-STAT3 in our clinical IHC laboratory (detailed procedures are in Supplementary Materials and Methods), which is certified under the provisions of the U.S. Clinical Laboratory Improvement Act. IHC procedures for cyclin E and Rb were reported previously (13) and also included in Supplementary Materials and Methods. IHC staining for γH2AX is as described previously (14) and briefly as follows: FFPE slides were deparaffinized, rehydrated, and boiled for 15 minutes in tris-based target retrieval solution (pH 9.0) and incubated for 10 minutes in 3% hydrogen peroxide. The sections were then blocked at room temperature for 30 minutes by using normal goat serum, and incubated in a humidified chamber overnight at 4°C with the primary antibody [rabbit-anti-phospho-histone H2AX (Ser139); Cell Signaling Technology] at a dilution of 1:100. The sections were then washed in PBS (3 × 5 minutes), incubated at room temperature with the secondary antibody (goat anti-rabbit) for 30 minutes, and with ABC for 15 minutes, using Vectastain Elite ABC Kit. Colors were developed with a DAB substrate (Vector Laboratories, Inc.). The sections were then counterstained with Mayer hematoxylin, dehydrated, and mounted. The evaluation of γH2AX on each slide was performed as the percentage of staining in the nuclei of tumor cells.

Statistical analysis

Each cell culture experiment was performed at least three times. Continuous outcomes were summarized with means and SDs. Comparisons among groups were analyzed by two-sided *t* test and Wilcoxon rank-sum test. These analyses were performed using SPSS software, version 12.0. The differences in expression of pre- and post-palbociclib treatment different biomarkers between groups were compared using either Wilcoxon (paired samples) one-sided test or McNemar test.

Integrative -omics analysis. For RNA-seq data, read counts from the nine T47D samples were normalized and $\log_2$ transformed using the variance stabilizing transformation method implemented in the R DESeq2 package (15). A subset of the normalized data was obtained by keeping only the significant differentially expressed genes (DEG) from the comparison of T47D parental versus T47D resistant (Clone2) and the samples that also have RPPA and mutation data available. On the basis of this subset of data, a hierarchical clustering heatmap was generated. The Pearson distance and the Ward minimum variance method were used for clustering. As for the significant DEGs, their association with the top 12 upregulated and top 12 downregulated gene sets from GSEA analysis was identified. Also incorporated was the RPPA data in terms of $\log_2$ normalized values for the samples that overlap with the RNA-seq data. A heatmap was produced similarly for the RPPA data based on the expression of proteins of interest except that the samples were not clustered but kept in the same order as the samples in the RNA-seq heatmap. In addition, the somatic mutation data from WES was also integrated. Mutations from the genes that belong to the top 12 upregulated and top 12 downregulated gene sets were selected. Among them, mutations with high, moderate, or low impact were kept for visualization.

Results

Palbociclib-resistant cells are cross-resistant to other CDK4/6 inhibitors and intrinsically resistant to endocrine therapy

We developed *in vitro* models of acquired resistance by treating MCF-7 and T47D cells with increasing concentrations of palbociclib (up to 5 μmol/L) in a step-wise manner over a 6 month period. Dose–response analysis revealed that the resistant cells are 9-fold more resistant to palbociclib and equally cross resistant to ribociclib and abemaciclib, as compared with parental cells (Fig. 1A). Clonogenic assay showed that palbociclib had no significant impact on the proliferation of MCF-7 and T47D resistant cells, while inducing a dose-dependent reduction in colony formation in parental cells (Fig. 1B). The resistant cells proliferated more slowly than the control cells in the absence of palbociclib (Fig. 1C; Supplementary Fig. S1A) however, increasing concentrations of all three CDK4/6 inhibitors, resulted in significant growth inhibition in the parental,

(*Continued.*) **C,** Cell counting every 3 days showing effect of 1 and 5 μmol/L palbociclib (Palbo) treatment for 6 days and recovery for 3 days on the proliferation of MCF-7 parental (Par) and resistant (Res) cells. **D,** Cell-cycle analysis by flow cytometry to examine the effect of palbociclib treatment (0.5–10 μmol/L) on MCF-7 and T47D parental (Par) and resistant (Res) cell lines. Conc, concentration. **E,** Western blot analysis showing levels of estrogen receptor (ERα) in MCF-7 parental (Par) and resistant (Res) cell lines (left). qPCR analysis shows mRNA levels of ERα in these cells (Par and Res; right). **F,** qPCR analysis shows mRNA levels of estrogen-responsive genes pS2, PR, and GREB1, transcription modulators of estrogen receptor GATA3 and NRIP1, and AR (left). Western blot analysis confirming downregulation of AR and PR in MCF-7 resistant cells (right). Par, parental; Res, resistant. **G,** Dose–response curves in MCF-7 and T47D parental (Par) and resistant (Res) cell lines after 24 hours estrogen deprivation then readdition of 10 nmol/L beta-estradiol (E2) and treatment of varying concentrations (conc; 0.01–12 μmoll/L) of tamoxifen (left) or fulvestrant (right). Dashed line depicts IC_{50} values. **H,** mRNA (top) and protein (bottom) analysis of FOXA1, a mediator of endocrine resistance. Par, parental; Res, resistant. For all graphs, error bars describe SD, and Student *t* test determined *P* values (*, $P < 0.05$; **, $P < 0.01$; ***, $P < 0.001$; Cnt, control).

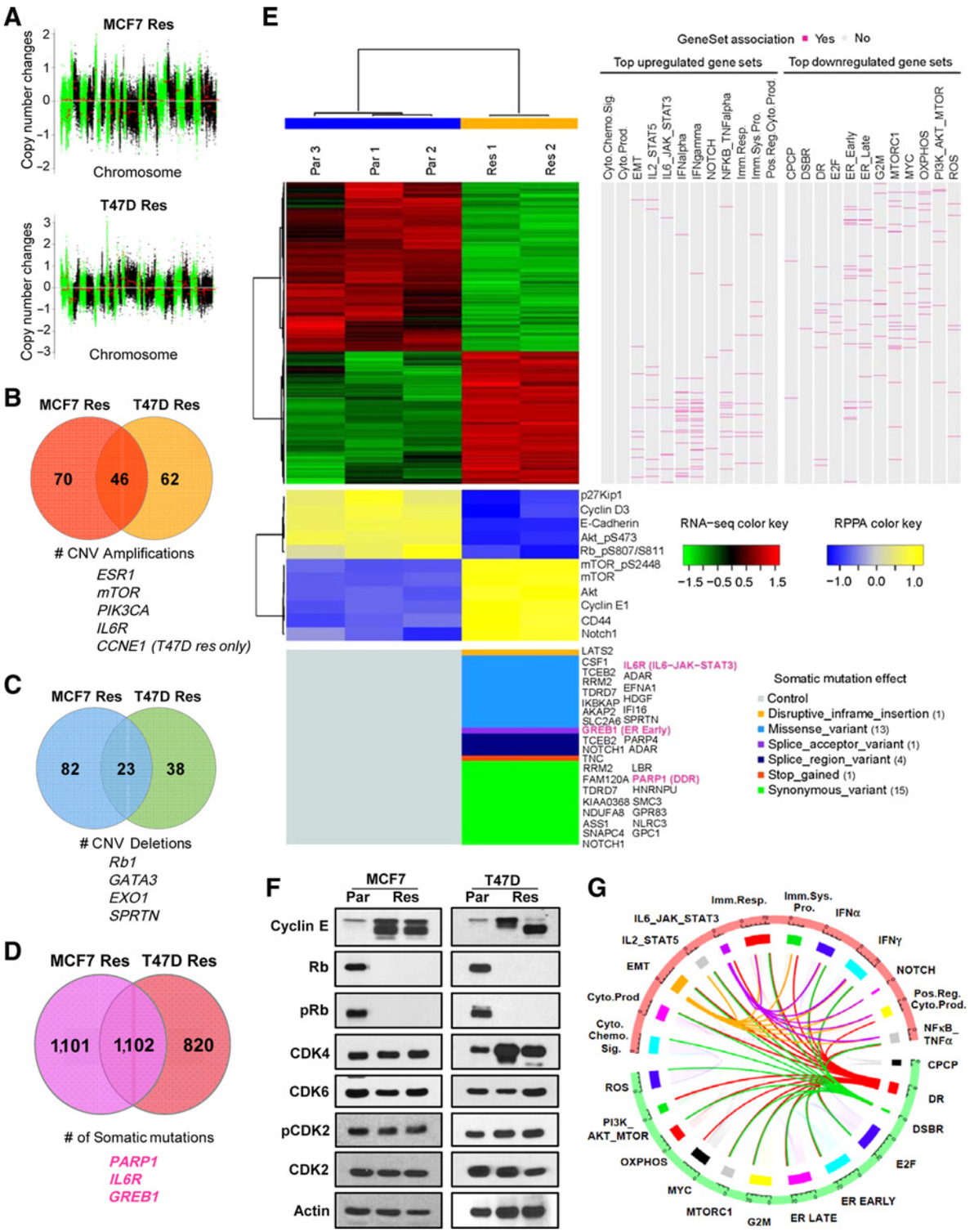

Figure 2.

Palbociclib-resistant cells have a distinct genomic, transcriptomic, and proteomic profile. **A,** Log_2 ratio for copy number changes in resistant (Res) cells only in comparison with parental cells, where the x-axis represents the chromosome location and chromosomes are separated by alternating green and black colors. Venn diagrams depicting the number of CNV amplifications (**B**) and number of CNV deletions (**C**) that are common between MCF-7– and T47D-resistant cells. **D,** Venn diagram representing the number of somatic mutations identified in the resistant (Res) cells. (*Continued on the following page.*)

but not resistant cells (Supplementary Fig. S1A–S1C). Moreover, compared with the parental cells, which were arrested in the G_1 phase of the cell cycle in response to the CDK4/6 inhibitors, the resistant cells did not arrest in any phase of the cell cycle following treatment with each of the three inhibitors (Fig. 1D; Supplementary Fig. S1D and S1E).

The palbociclib-resistant cells were also resistant to endocrine therapy. Immunoblot and qPCR analysis revealed that ERα protein levels were undetectable, whereas mRNA was downregulated in the palbociclib-resistant cells relative to parental cells (Fig. 1E). The mRNAs encoding the estrogen-responsive genes pS2, PR (PgR/PR), and GREB1, as well as transcription modulators of ER GATA3 and NRIP1, and androgen receptor (AR) were significantly downregulated (Fig. 1F) in the palbociclib-resistant cells. PR and AR protein levels were also undetectable in the resistant cells (Fig. 1F; Supplementary Fig. S1F). Furthermore, the palbociclib-resistant clones were resistant to endocrine therapy as treatment with tamoxifen or fulvestrant increased the IC_{50} of tamoxifen by 16-fold and that of fulvestrant by 13- to 17-fold in MCF-7– and T47D-resistant cells (Fig. 1G). Previous studies have reported upregulation of FOXA1 as a potential driver of endocrine resistance in ER-positive metastatic disease (16–18), which we also assessed; qPCR analysis depicted upregulation of FOXA1 mRNA in the resistant cells as compared with parental cells (Fig. 1H; $P < 0.001$ and $P < 0.01$) without changes in its protein levels (Fig. 1H; Supplementary Fig. S1G). Downregulation of FOXA1 by RNA interference revealed a further reduction in ER mRNA levels in the resistant cells (Supplementary Fig. S1H and S1I), without any subsequent reduction in ER target genes (Supplementary Fig. S1J). We also examined the role of the glucocorticoid receptor (GR) and aryl hydrocarbon receptor (AhR) in the resistant cells as increased activity of GR and/or AhR is emerging as important mediators for promoting cell survival in ER-negative or ER-suppressed breast cancers (19, 20). However, no changes were detected in GR and AhR mRNA levels between parental and resistant cells (Supplementary Fig. S1K). In addition, treatment of parental and resistant cells with mifepristone (RU486), an inhibitor of GR and PR and to a lesser extent AR, revealed a 2-fold decreased sensitivity to RU486 in resistant (IC_{50} 11.7 μmol/L) compared with parental cells (IC_{50} 5.8 μmol/L; Supplementary Fig. S1L). Collectively, these studies suggest that palbociclib-resistant cells not only are cross resistant to other CDK4/6 inhibitors but are also resistant to endocrine therapy.

Palbociclib-resistant cells have a distinct genomic, transcriptomic, and proteomic profile

To help decipher specific mechanisms of resistance to palbociclib, we performed multi-omics analysis on the resistant cells as compared with parental cells. WES revealed similar genomic copy number changes in the MCF-7– and T47D-resistant cells, when compared with the parental cells and as presented in copy-number variation (CNV) plots showing either amplification or deletion across different chromosomes (Fig. 2A; Supplementary Table S1). Comparison of the CNVs among MCF-7– and T47D-resistant cells also exhibited amplifications in the chromosome regions that harbor the *ESR1* gene and *CCNE1*, and deletion in the region of *Rb1* (Fig. 2B and C; Supplementary Table S1). Despite the amplification of *ESR1* gene, *ESR1* gene mutations were not included among the 2,000 somatic mutations identified in the resistant cells (Fig. 2D; Supplementary Table S2).

RNA-seq analysis identified 2,836 DEGs in resistant cells (Fig. 2E; Supplementary Table S3) compared with parental cells. GSEA-depicted estrogen response and DNA repair pathways were significantly downregulated, whereas epithelial–mesenchymal transition (EMT) and stem-like pathways (IL6/STAT3, Notch, and Wnt) were significantly upregulated (Fig. 2E; Supplementary Table S4). Several gene mutations identified by WES overlapped with gene expression changes within the top 12 up- and down-regulated pathways (Fig. 2E), suggesting functional consequences of these mutations. Finally, proteomic analysis performed by RPPA identified 77 proteins that were significantly different between resistant and parental cell lines (Supplementary Table S5) with cyclin E, mTOR, phospho-mTOR, Akt, Notch1, and CD44 among the upregulated proteins, whereas E-cadherin, phospho-Rb (p-Rb), p27, p-Akt, and cyclin D3 among the down-regulated proteins in the resistant cells (Fig. 2E). As such, there is concordance among the genomic, transcriptomic, and proteomic analysis for the pathways altered in the resistant cells. Immunoblot blot analysis validated the downregulation of Rb and p-Rb, as well as induction of low-molecular-weight isoforms of cyclin E (LMW-E) in the resistant cells (Fig. 2F). However, expression of CDK4/6 and phospho-CDK2 remained unchanged (Fig. 2E and F). To determine CDK2- and cyclin E–associated kinase activity, two independent *in vitro* kinase assays revealed that although CDK2 kinase activity is similar between parental and resistant cells (Supplementary Fig. S2A), that cyclin E–associated activity is increased in the MCF-7–resistant cells, which have endogenously higher levels of cyclin E protein (Supplementary Fig. S2B).

(*Continued.*) **E,** Illustration of integrative analysis. A hierarchical clustering heatmap was generated for the normalized RNA-seq data based on the significant DEGs from the comparison of T47D parental (Par) versus T47D-resistant (Res) cells (clone2). The Pearson distance and the Ward minimum variance method were used for clustering both genes and samples. Red and green colors indicate increased and decreased expression levels, respectively, in the standardized scale. On the right side of the heatmap, association of the genes in the heatmap with the top 12 upregulated and top 12 downregulated gene sets from GSEA analysis is identified. Genes that belong to each gene set are highlighted in deep pink. The heatmap for the normalized RPPA data is plotted below the heatmap for the RNA-seq data. Proteins were clustered in the same way, whereas the samples were not clustered but kept in the same order. Yellow and blue colors indicate increased and decreased expression levels, respectively, in the standardized scale. Plotted on the bottom are somatic mutations from the genes that belong to the pathways of interest. Mutation effects are indicated by different colors. Three genes of interest (GREB1, IL6R, and PARP1) are colored in deep pink. **F,** Western blot analysis showing levels of cyclin E, Rb, pRb, CDK4, CDK6, phosphorylated CDK2 (pCDK2), and CDK2 in MCF-7 and T47D parental (Par) and resistant (Res) cells. **G,** Circos plot based on the number of genes in each of the 12 upregulated (red) and 12 downregulated (green) pathways and the number of genes shared by each pathway. Breadth of the connecting ribbons in the Circos plot is proportional to the fraction of genes shared between each pathway. CPCP, cellular protein catabolic process; Cyto. Chemo. Sig., cytokine chemokine signaling; Cyto. Prod., cytokine production; DR, DNA repair; E2F, E2F targets; ER_EARLY, estrogen response early; ER_LATE, estrogen response late; G2M, G2M checkpoint; IFNα, interferon alpha response; IFNγ, interferon gamma response; Imm. Resp., immune response; IL2_STAT5, IL2/STAT5 signaling; IL6_JAK_STAT3, IL6/JAK/STAT3 signaling; Imm. Sys. Pro., immune system process; MTORC1, MTORC1 signaling; MYC, MYC targets V1; NFB_TNFa, TNFa signaling via NFB; NOTCH, NOTCH signaling; OXPHOS, oxidative phosphorylation; PI3K_AKT_MTOR, PI3K/AKT/MTOR signaling; Pos. Reg. Cyto. Prod., positive regulation of cytokine production; ROS, reactive oxygen species.

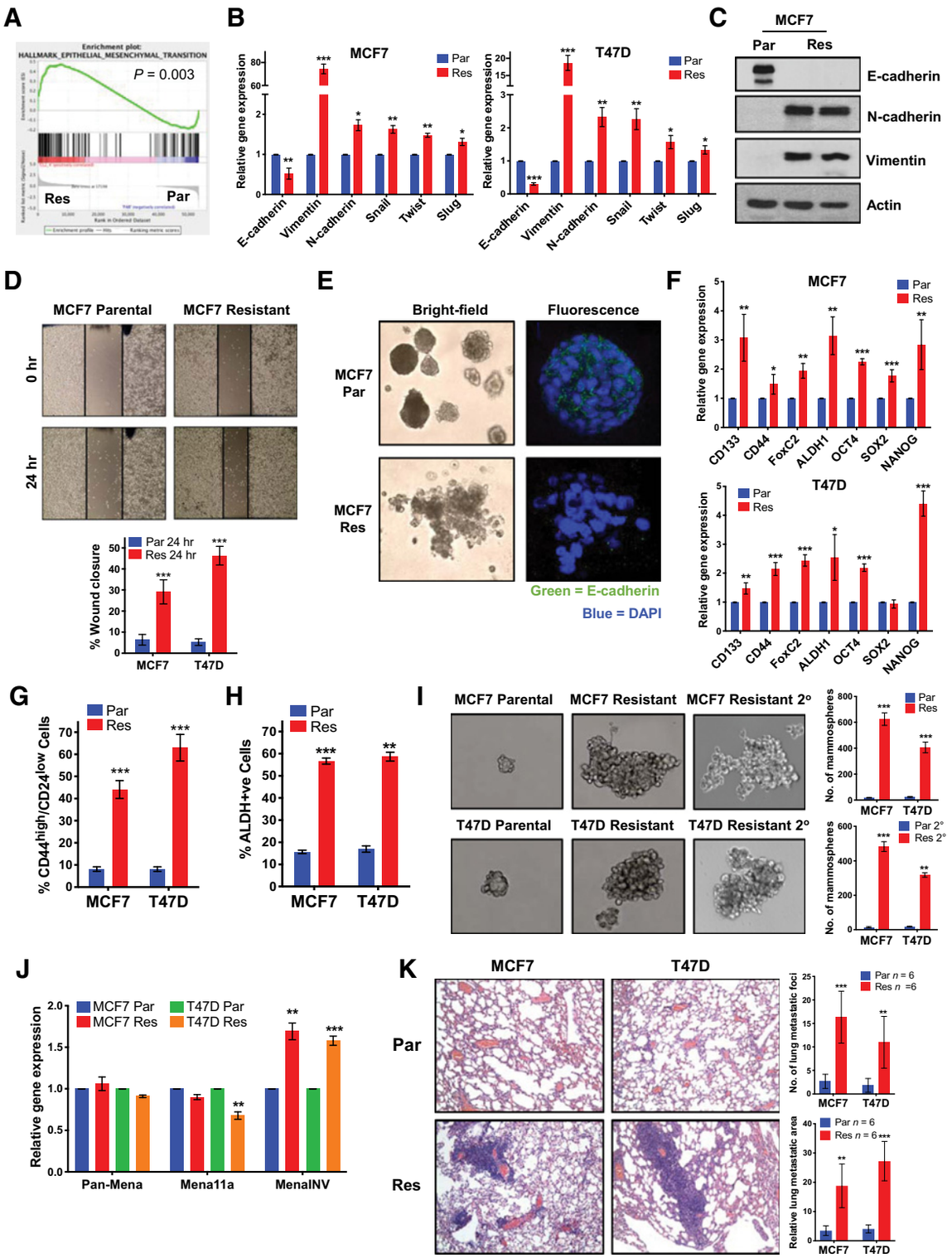

Figure 3.

Upregulation of EMT and B-CSC-L pathways in palbociclib-resistant cells increases migratory and invasive capacity, leading to increased metastasis *in vivo*. **A,** GSEA enrichment plot of EMT. Par, parental; Res, resistant. **B,** Increased mRNA expression of EMT markers in the palbociclib-resistant (Res) compared with parental (Par) in MCF-7 and T47D cell lines. **C,** Western blots show increased protein expression of EMT markers (N-cadherin and vimentin) and decreased expression of E-cadherin in MCF-7–resistant (Res) cell lines. Par, parental. (*Continued on the following page.*)

Treatment of parental and resistant cells by pan-CDK inhibitors: dinaciclib, roscovitine, and SNS-032 revealed increased sensitivity of the resistant cells to dinaciclib and SNS-032 (Supplementary Fig. S2C and S2D), suggesting increased functionality of other CDKs, besides CDK2, in the resistant cells.

These analyses also illustrated that genes within the mTOR and PI3K growth signaling pathway were amplified in the palbociclib-resistant cells. Treatment of parental and resistant cells with inhibitors against PI3K or mTOR revealed that although there was no difference in response of parental and resistant cells to BKM120 (pan-Class I PI3K inhibitor; Supplementary Fig. S2E), the resistant cells were less sensitive to everolimus (mTOR inhibitor) as compared with parental cells (Supplementary Fig. S2F and S2G). However, treatment of both parental and resistant cells by everolimus caused downregulation of p-mTOR/mTOR and pS6/S6 (downstream target of mTOR) proteins (Supplementary Fig. S2H), suggesting that the inhibitor is reaching its targets. Because Rb status has recently been implicated in the suppression of mTOR signaling (21), we also treated MCF7 cells with shRNA knockdown of Rb (Supplementary Fig. S2I) and observed that Rb deficiency leads to decreased sensitivity to everolimus (Supplementary Fig. S2J). Collectively these results suggest that the lack of sensitivity of the palbociclib-resistant cells to mTOR inhibition may be in part due to downregulation of Rb that is observed in the resistant cells.

To facilitate the identification of potential targetable pathways from the GSEA results, beyond current clinically used targeted therapies, we examined the coordinately upregulated and downregulated subsignatures contained within the high scoring GSEA results by generation of a Circos plot (Fig. 2G). The breadth of the connecting ribbons in the Circos plot is proportional to the fraction of genes shared between each pathway. Out of the top upregulated pathways in resistant cells, EMT and stem-like pathways overlapped with the IL6/JAK/STAT3 pathway, suggesting that targeting any of these pathways may have inhibitory activity on the other. Among the key downregulated pathways, DNA repair and double-strand break repair (DSBR) pathways overlapped with several of the other top GSEA pathways, but not with the IL6/JAK/STAT3 pathway. Targeting divergent pathways allows for the possibility in increasing cancer cell death while reducing the likelihood of drug resistance.

Upregulation of EMT and stem-like pathways in palbociclib-resistant cells increases their migratory and invasive capacity, leading to increased metastasis *in vivo*

Because the GSEA analysis implicates upregulation of EMT (Fig. 3A) and pathways that promote stem-like properties (IL6/JAK/STAT3 and Notch; Fig. 2E) in the palbociclib-resistant cells, we next examined whether resistant cells have acquired an EMT and/or a stem-like phenotype. mRNA levels in the resistant cells showed a significant decrease in the epithelial marker E-cadherin, a significant increase in the mesenchymal markers vimentin and N-cadherin, and a significant increase in the EMT transcription factors Snail, Twist, and Slug (Fig. 3B). Immunoblot analysis validated the expression of EMT proteins, confirming an increase in N-cadherin and vimentin and decrease in E-cadherin in resistant cells relative to parental cells (Fig. 3C; Supplementary Fig. S3A). This EMT signature correlates with a highly migratory and invasive phenotype, as predicted by GSEA analysis (Supplementary Fig. S3B), and confirmed by the migratory ability of the resistant cells via scratch assay, which revealed a higher percentage of wound closure compared with parental cells (Fig. 3D; Supplementary Fig. S3C). Moreover, we observed loss of apico-basal polarity in the palbociclib-resistant cells, as predicted by GSEA (Supplementary Fig. S3D), visualized by the lack of coherent acini formation and the loss of E-cadherin staining on the basal surface in comparison with parental cells (Fig. 3E; Supplementary Fig. S3E) supporting invasive behavior.

To interrogate the stem-like phenotype of resistant cells, we examined mRNA expression of stem-like markers and transcription factors, including CD133, CD44, FoxC2, ALDH1, OCT4, SOX2, and NANOG, all of which showed significant upregulation in the palbociclib-resistant cells compared with parental cells (Fig. 3F). Flow cytometry analysis also showed that the resistant cells have a significant increase in the $CD44^{high}/CD24^{low}$ (Fig. 3G; Supplementary Fig. S3F) and ALDH-positive population (Fig. 3H; Supplementary Fig. S3G) compared with the parental cell lines, which have been previously implicated as markers for breast cancer stem-like cells (B-CSC-L; refs. 22, 23). Finally, mammosphere assays, another B-CSC-L indicator (24), illustrated that the MCF-7 and T47D palbociclib-resistant cells formed larger and greater numbers of mammospheres in the primary and secondary mammosphere assays, compared with parental cells (Fig. 3I).

To interrogate whether the resistant cells also have characteristics of metastatic spread, we examined the expression of Mena, an isoform of actin-regulatory protein and a member of the Ena/VASP family of proteins and MenaINV, which is as a key marker of metastatic risk and poor clinical outcome (25–27). During tumor progression, Mena is alternatively spliced to produce multiple functionally distinct isoforms: Mena (Pan-Mena), MenaINV, and Mena11a. mRNA levels of different Mena isoforms showed that the palbociclib-resistant cells contained significantly increased amounts of MenaINV in comparison with parental cells (Fig. 3J), predicting their increased metastatic potential. To directly examine the metastatic potential of palbociclib-resistant cells, we carried out tail vein injection of MCF-7– and T47D-resistant and parental cells in nude mice and found that the palbociclib-resistant cells have increased lung metastatic foci, as visualized by H&E and quantified by number and relative area (Fig. 3K). Collectively, our analyses show that palbociclib-resistant breast cancer cells have increased

(*Continued.*) **D,** Scratch wound healing assay displays increased cell migration after 24 hours (hr) in the resistant (Res) cells. Par, parental. **E,** Acini formation in MCF-7 parental (Par) and resistant (Res) cells after 15 days in 3D culture shown by bright-field and fluorescent immunostained with E-cadherin (green) and nuclei counterstained with DAPI (blue). **F,** Increased gene expression of transcription factors related to dedifferentiation in MCF-7– and T47D-resistant (Res) cell lines. Par, parental. **G,** Increased B-CSC-L population observed in the resistant cells as identified by $CD44^{high}/CD24^{low}$. Par, parental; Res, resistant. **H,** Resistant cells have an increase in aldehyde dehydrogenase (ALDH)–positive cells, an additional marker for B-CSC-L population. Par, parental; Res, resistant. **I,** Mammosphere formation after 6 days and secondary (2°) mammosphere formation by the resistant (Res) cells show the B-CSC-L features of the cells. Par, parental. **J,** Increased gene expression of MenaINV, a prometastatic factor, compared with the nonmetastatic isoforms, Pan-Mena and Mena11a, in resistant (Res) cells. Par, parental. **K,** Representative H&E images (left) and quantified number (top right) and area (bottom right) of lung metastasis in nude mice 10 weeks following tail vein injection with 10^6 MCF-7 and T47D parental (Par) and resistant (Res) cells. For all graphs, error bars describe SD, and Student *t* test determined *P* values.

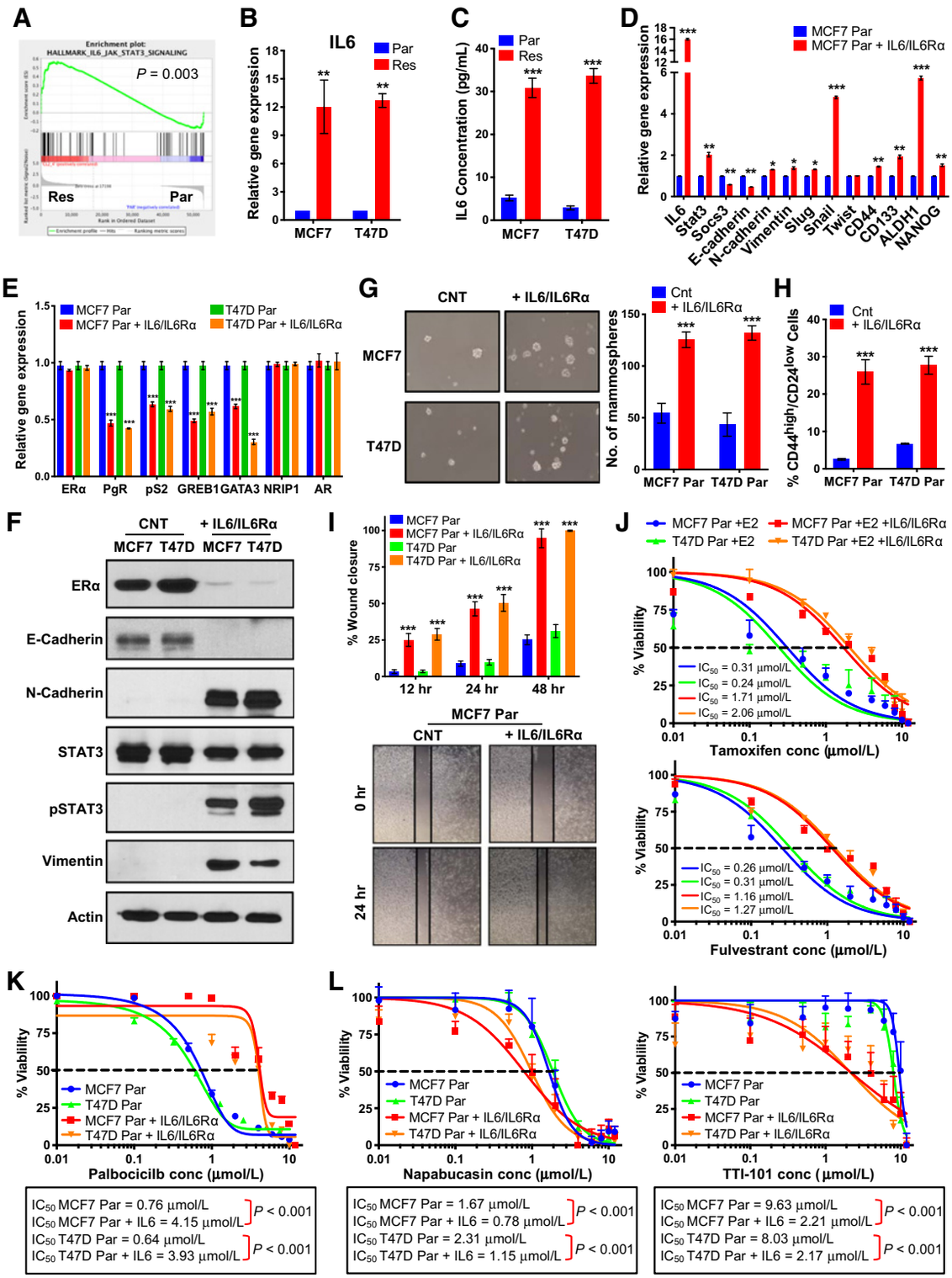

Figure 4.

Regulation of the ER by IL6/STAT3 promotes resistance to endocrine therapy and palbociclib. **A,** GSEA enrichment plot of IL6_JAK_STAT3 signaling indicating increased signaling in resistant (Res) cells. Par, parental. **B,** qRT-PCR analysis of IL6 shows 10-fold increase in MCF-7– and T47D-resistant (Res) cells compared with parental (Par) cells. **C,** IL6 ELISA on media collected from MCF-7 and T47D parental (Par) and resistant (Res) cells cultured for 3 days shows a 20-fold increase in MCF-7– and T47D-resistant cells compared to parental cells. (*Continued on the following page.*)

EMT markers and an enhanced B-CSC-L phenotype, accompanied by elevated migratory and invasiveness activity.

Regulation of the ER by IL6/STAT3 promotes resistance to palbociclib

Circos plot analysis (Fig. 2G) showed that EMT and stem-like pathways overlap with IL6/STAT3 pathways, whereas GSEA and WES exhibited enrichment and amplification of IL6R (Figs. 2B and 4A) in resistant cells. Because ERα negatively regulates IL6 (28) and, conversely, IL6 induction negatively regulates ERα (29), we next asked whether induction of IL6 in the palbociclib-resistant cells leads to downregulation of ERα and subsequent lack of response to endocrine therapy. IL6 mRNA levels and IL6 protein secreted into the media exhibited a >10- and >20-fold increase, respectively, in the palbociclib-resistant compared with parental cells (Fig. 4B and C). To interrogate the role of IL6 in modulating EMT, B-CSC-L, migration, ERα levels, and response to endocrine therapy and palbociclib, we subjected the parental (palbociclib-sensitive) cells to exogenous IL6 treatment. Initially, we determined the lowest concentration of exogenous IL6 (0.5 ng/mL) to add to cells that induced comparable mRNA levels of IL6 and STAT3 as those in resistant cells (Fig. 4D; Supplementary Fig. S4A and S4B). Treatment of sensitive cells with IL6 induces EMT/B-CSC-L markers (Fig. 4D; Supplementary Fig. S4B) and downregulation of ER signaling as observed in the palbociclib-resistant cells (Fig. 4E). EMT markers and ERα protein levels are also downregulated in response to IL6 treatment (Fig. 4F). Moreover, the B-CSC-L features of the parental cells treated with IL6 were confirmed by mammosphere formation (Fig. 4G) and increase in $CD44^{high}/CD24^{low}$ enriched cell population (Fig. 4H; Supplementary Fig. S4C). IL6 treatment of the parental cells also resulted in an increase in cell migration (Fig. 4I; Supplementary Fig. S4D), which is not due to an increase in cell proliferation (Supplementary Fig. S4E). We next assessed whether the IL6-treated parental cells are responsive to endocrine therapy, and found that these cells are 5-fold more resistant to tamoxifen and 7-fold more resistant to fulvestrant compared with cells not treated with IL6 (Fig. 4J). Moreover, dose–response studies with palbociclib showed that the parental cells treated with IL6 are 5-fold more resistant to palbociclib treatment compared with the cells cultured in the absence of IL6 (Fig. 4K). In addition, based on a previous study suggesting the role of cytokine signaling in FOXA1 upregulation and endocrine resistance (17), we observed FOXA1 is also induced in parental cells treated with IL6 (Supplementary Fig. S4F). Finally, we examined the effects of STAT3 inhibition on the cell viability of the parental cells treated with IL6, because increased protein levels of tyrosine-phosphorylated STAT3 (pY-STAT3) is the canonical downstream effector of IL6 (Fig. 4F). Parental IL6-treated cells were significantly more sensitive to inhibitors of STAT3 (napabucasin and TTI-101; Fig. 4L). Sensitivity to TTI-101 was greater due in part to inhibition of STAT5 (30), as evident by increased pY-STAT5 levels in IL6-treated parental cells (Supplementary Fig. S4G). These results suggest that targeting STAT3 may have therapeutic benefit in the palbociclib-resistant setting.

IL6 drives the JAK/STAT pathway to promote EMT and B-CSC-L characteristics in palbociclib-resistant cells

IL6, through the activation of JAK, leads to the phosphorylation of STAT3 on tyrosine (Y) residue 705 (31) and to some extent activation of STAT5 (32). We observed that pY-STAT3 and pY-STAT5 protein levels were significantly increased in the resistant cells compared with an almost undetectable level in the parental cells (Fig. 5A; Supplementary Fig. S5A and S5B). STAT3 and STAT5a/b mRNA levels are significantly induced by in the palbociclib-resistant cells compared with the parental cells (Fig. 5B; Supplementary Fig. S5C). Because JAK has a direct role in the activation of STAT3 and 5, by mediating tyrosine phosphorylation, we asked whether palbociclib-resistant cells were sensitive to a JAK inhibitor. Dose–response assays showed that palbociclib-resistant cells are 5- to 10-fold more sensitive to the JAK inhibitor tofacitinib versus parental cells (Supplementary Fig. S5D). In addition, decreased mRNA expression of a negative regulator JAK, SOCS3, was observed in palbociclib-resistant cells (Fig. 5C). Collectively, our results suggest that IL6 induction in palbociclib-resistant cells leads to STAT3 and STAT5 activation.

To interrogate whether STAT3 is a viable target in the resistant cells, we treated the parental and the resistant cells with two known STAT3 inhibitors, Stattic (33) and TTI-101 (34), and one inhibitor of cancer stem cells, napabucasin (35, 36). Dose–response curves with Stattic, which inhibits activation, dimerization, and nuclear translocation of STAT3, showed only modest activity in resistant cells (Supplementary Fig. S5E). However, dose–response curves with napabucasin (shown in gel shift assays to decrease STAT3 binding to DNA) and TTI-101 (a direct inhibitor of STAT3 that targets the pY-peptide binding pocket within its SH2 domain) decreased cell viability of the MCF-7– and T47D-resistant cells by 2.5- and >25-fold, respectively (Fig. 5D and E). TTI-101 treatment of the resistant cells resulted in downregulation of p-STAT3 and to a lesser extent p-STAT5 (Supplementary Fig. S5F). The IL6/STAT3 pathway has been shown to be preferentially expressed within the $CD44^{high}/CD24^{low}$ population of breast cancer cells, suggesting its role in B-CSC-L enrichment (37). Measurement of $CD44^{high}/CD24^{low}$-enriched cells and mammospheres revealed treatment of the resistant cells with both agents (napabucasin and TTI-101) significantly decreased: (i) the $CD44^{high}/CD24^{low}$ B-CSC-L population (Fig. 5F and G), (ii)

(*Continued.*) **D,** Increased mRNA expression of EMT markers and transcription factors related to B-CSC-L markers in the parental (Par) cells treated with 0.5 ng/mL IL6 and 0.125 ng/mL IL6Rα (i.e., IL6/IL6Rα) for days compared with untreated parental in MCF-7 cell lines. **E,** qPCR analysis shows mRNA levels of estrogen-responsive genes pS2, PR (PgR), and GREB1, transcription modulators of ER GATA3 and NRIP1, and AR in parental (Par) cells treated with IL6/IL6Rα in MCF-7 and T47D cell lines. **F,** Western blot analysis show levels of ERα, EMT markers, and STAT3 activation in IL6/IL6Rα-treated parental cells. CNT, control. **G,** Mammosphere formation is increased in the parental cells treated with IL6/IL6Rα. CNT, control. **H,** Increased B-CSC-L population observed in the parental (Par) cells treated with IL6/IL6Rα as identified by $CD44^{high}/CD24^{low}$. Cnt, control. **I,** Scratch wound healing assay displays increased cell migration after 12, 24, and 48 hours (hr) in the parental (Par) cells treated with IL6/IL6Rα. CNT, control. **J,** Dose–response curves in MCF-7 and T47D parental (Par) cells treated with IL6/IL6Rα after 24 hours estrogen deprivation then readdition of 10 nmol/L beta-estradiol (E2) with varying concentrations (conc) of tamoxifen (top) or fulvestrant (bottom). **K,** Dose–response curves show resistance to increasing doses of palbociclib (0.01–12 μmol/L) for 6 days and recovery for 6 days in the parental cells treated with IL6/IL6Rα. conc, concentration. **L,** Dose–response curves with TTI-101 (right) and napabucasin (left) showing increased sensitivity to STAT3 inhibition in parental (Par) cells after treatment with recombinant IL6/IL6Rα. conc, concentration.

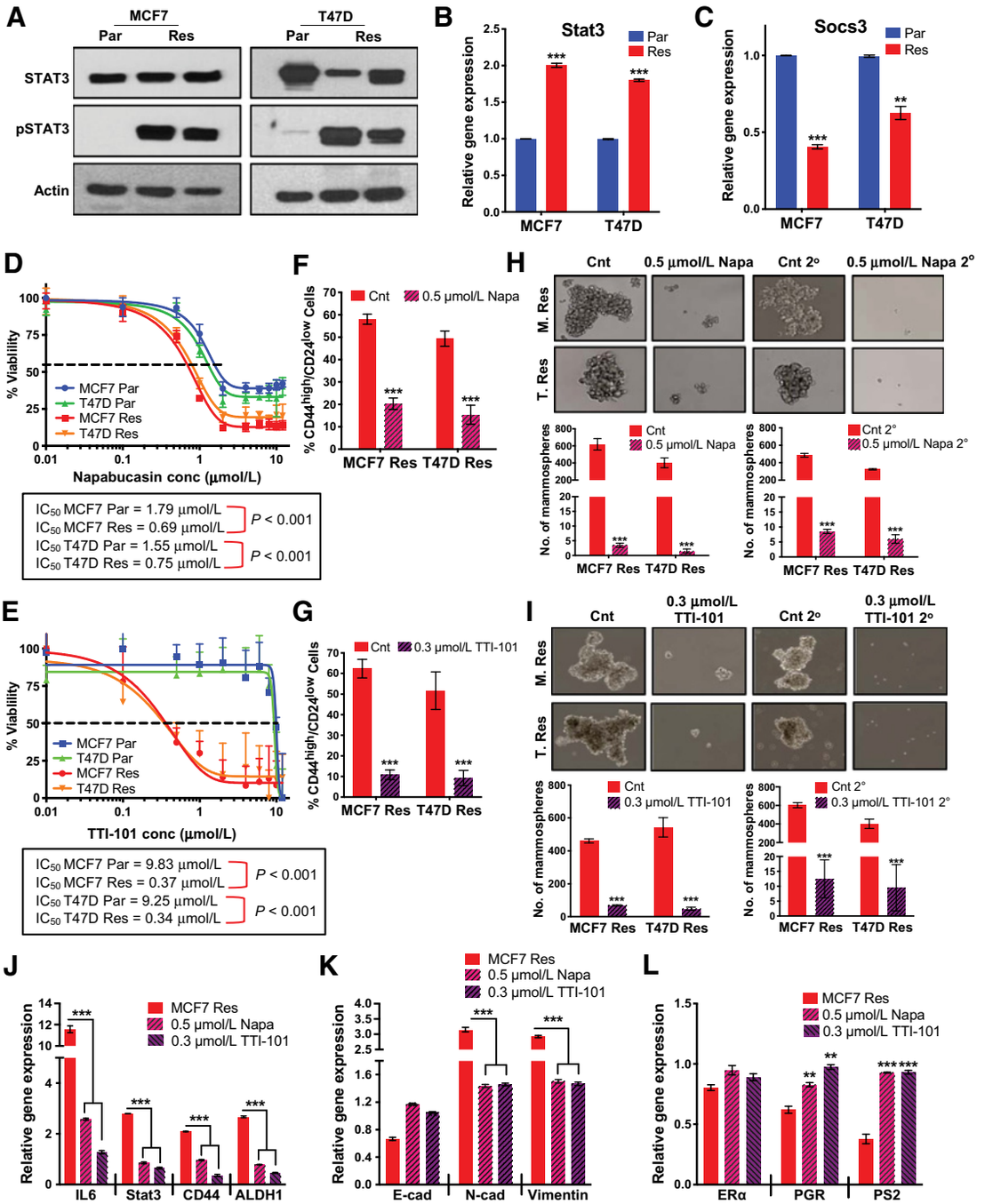

Figure 5.

IL6 drives the STAT3 pathway to promote EMT and B-CSC-L population in palbociclib-resistant cells. **A,** Western blot analysis shows that total STAT3 levels do not change, but pY-STAT3 levels increase in the MCF-7– and T47D-resistant (Res) cells. Par, parental. **B,** STAT3 mRNA levels are increased 2-fold in the resistant (Res) compared with parental (Par) cells. **C,** mRNA levels of the negative regulator of IL6 cytokine signaling via JAK/STAT3, SOCS3, is significantly downregulated in the resistant cells. Dose–response curve of varying concentrations of napabucasin, a cancer stemness inhibitor via STAT3 (**D**), and TTI-101, a STAT3 inhibitor blocking phosphorylation (**E**), for 3 days and recovery for 9 days. Treatment with 0.5 μmol/L napabucasin (**F**) and 0.3 μmol/L TTI-101 (**G**) for 3 days significantly decreases the B-CSC-L ($CD44^{high}/CD24^{low}$) population in the resistant cells. Mammosphere formation in the resistant cells is blunted by treatment with 0.5 μmol/L napabucasin (**H**) and 0.3 μmol/L TTI-101 (**I**). Cnt, control; conc, concentration; Napa, napabucasin; Par, parental; Res, resistant. **J,** mRNA analysis of IL6/STAT3 signaling and cancer stem cell factors, CD44 and ALDH, after treatment with 0.5 μmol/L napabucasin (Napa) and 0.3 μmol/L TTI-101 for 3 days. **K,** Decreased mRNA expression of EMT markers [N-cad herin (N-cad) and vimentin] and increased expression of E-cadherin (E-cad) in the palbociclib-resistant cells after treatment with 0.5 μmol/L napabucasin (Napa) and 0.3 μmol/L TTI-101 for 3 days. **L,** mRNA expression of ERα and estrogen-responsive genes in the resistant cells after treatment with 0.5 μmol/L napabucasin (Napa) and 0.3 μmol/L TTI-101 for 3 days. For all graphs, error bars describe SD, and Student *t* test determined *P* values. Cnt, control.

primary and secondary mammosphere formation (Fig. 5H and I), (iii) IL6/STAT3 and STAT5 signaling and B-CSC-L markers (i.e., CD44 and ALDH; Fig. 5J; Supplementary Fig. S5G), and (iv) the EMT pathway (Fig. 5K). Pharmacologic inhibition of STAT3 also resulted in the expression (i.e., rescue) of the ER target genes, *PgR* and *PS2*, in the palbociclib-resistant cells (Fig. 5L). Downregulation of FOXA1 (Supplementary Fig. S1H), however, does not alter mRNA levels of EMT/B-CSC-L markers or the $CD44^{high}/CD24^{low}$ population in the resistant cells (Supplementary Fig. S5H and S5I). Finally, shRNA knockdown of STAT3 in MCF-7–resistant cells, which resulted in downregulation of both STAT3 mRNA and protein expression (Supplementary Fig. S5J and S5K), also resulted in a significant decrease in the B-CSC-L population (Supplementary Fig. S5L). Collectively, these results suggest not only that the IL6/STAT3 pathway plays a crucial role in driving B-CSC-L population in palbociclib-resistant cells, but also that inhibition of STAT3 may provide a novel therapeutic option for these enriched B-CSC-L palbociclib-resistant cells.

DNA repair deficiency in palbociclib-resistant cells sensitizes cells to PARP and Wee1 inhibition, which act synergistically with STAT3 inhibitors

We next examined DNA repair and double-strand break (DSB) repair pathways in the palbociclib-resistant cells as these two pathways (i) were among the top downregulated pathways identified from RNA-seq and GSEA analysis (Fig. 2E; Supplementary Fig. S6A) and (ii) depicted by the Circos plot analysis (Fig. 2G) to be divergent from IL6/STAT3 pathways. Here, we propose that targeting divergent pathways allows for the possibility of synergistic cell death in the palbociclib resistant, but not sensitive cells.

Expression of key DSBR genes, *Rad51*, *BRCA1*, and *BRCA2*, were significantly decreased in palbociclib-resistant MCF-7 and T47D cells, compared with parental cells. (Supplementary Fig. S6B). IF staining of γH2AX foci depicted a 5-fold increase in the number of DNA DSBs in the resistant cells as compared with parental cells (Fig. 6A). Deficiency in the repair of these DSBs was visualized by Rad51 staining (Fig. 6A), implying that palbociclib-resistant cells have less DNA repair activity compared with parental cells. Quantitation of the ratio of γH2AX to Rad51 revealed that the resistant cells have an 8- to 10-fold increase in unrepaired DNA damage compared with parental cells (Fig. 6A). Treatment of the resistant cells with various DNA-damaging reagents: irradiation, cisplatin, and doxorubicin showed increased sensitivity to irradiation therapy but not cisplatin or doxorubicin treatment (Fig. 6B and C). Moreover, the sensitivity of the resistant cells to the PARP inhibitors, olaparib and niraparib, revealed significant dose-dependent reduction in cell viability in the palbociclib-resistant cells compared with parental cells (Fig. 6D; Supplementary Fig. S6C). A similar response was seen with the Wee1 kinase inhibitor AZD1775, shown previously to induce genomic instability (38), where the palbociclib-resistant cells exhibit increased sensitivity (Fig. 6E). However, as expected, treatment with the PARP inhibitors or the Wee1 kinase inhibitor did not affect the B-CSC-L population in the resistant cells (Supplementary Fig. S6D), indicating these drugs may be targeting the proliferation of the non-B-CSC-L population, whereas STAT3 inhibitors target the B-CSC-L population in the palbociclib-resistant cells.

To examine the synergy between PARP inhibition and STAT3 inhibition, we used a high-throughput survival assay that allows comprehensive evaluation of two or more drugs followed by determination of the combination index (CI). The CI, based on the Chou-Talalay method for drug combination (39), determines the degree of synergy ($CI < 0.9$), additivity ($CI = 0.9–1.1$), or antagonism ($CI > 1.1$) of the interaction of two drugs being tested (40). Results indicated that the combination of napabucasin and olaparib was highly synergistic with CI values of 0.13 and 0.26, and additive for TTI-101 and olaparib with CI values of 0.97 and 0.92 in the MCF-7– and T47D-resistant cells, respectively (Fig. 6F). Furthermore, the combination of olaparib and napabucasin or TTI-101 significantly decreased colony formation as compared with no treatment or single-drug treatments (Fig. 6G and H). Finally, combined treatment with olaparib and napabucasin or TTI-101 increased cell death via apoptosis in the palbociclib-resistant cells (Fig. 6I; Supplementary Fig. S6E). Flow cytometric analysis examining the percent of apoptotic cells that are enriched in B-CSC-L as compared with the non-B-CSC-L population revealed that combination inhibition of PARP and STAT3 diminishes both cell populations better than either single agent in the palbociclib-resistant cells (Fig. 6J). The same survival assay analysis was performed with the combination of AZD1775 and STAT3 inhibitors. Results indicated synergism between drug combinations targeting the STAT3 and DNA damage/repair pathways, decreased colony formation, and increased apoptosis (Supplementary Fig. S6G–S6K). Collectively, these results suggest that combined treatment with STAT3 and PARP inhibitors or Wee1 kinase inhibitor is an effective treatment strategy for palbociclib-resistant cells.

Analysis of pre/post-palbociclib treatment in samples from patient with metastatic ER-positive breast cancer identifies potential biomarkers of acquired resistance

Despite preclinical results suggesting that Rb, cyclin D, and p16 status predict response to palbociclib (41–43), results from clinical trials showed no significant correlation between response and expression of these markers (44, 45), nor mutational status of *PIK3CA* or *ESR1* (46), leaving no established clinically useful predictive biomarkers (47). We have begun to address this void by translating our *in vitro* findings to patient samples and interrogating whether the pathways that are altered in the palbociclib-resistant cells (Fig. 2) are also altered in tumor samples from patients who have developed resistance to palbociclib (Fig. 7).

Specifically, we asked whether the protein expression of ER, cyclin E, γH2AX, pY-STAT3, or phosphorylated Rb (pRb) can identify those patients who have developed resistance to palbociclib treatment. The rationale for choosing these markers was based on our preclinical multi-omics analysis (Fig. 2) and subsequent validation of the deregulation of each of these markers (Figs. 1, 3–6). Cyclin E was included in these analysis due to its role in inducing replicative stress and DNA damage (9, 48–50) and because our previous studies where we examined tumor samples from a cohort of 109 patients with ER-positive, HER-2 negative advanced breast cancer treated with combination of letrozole or fulvestrant with palbociclib at MDACC revealed that patients with the tumor-specific cytoplasmic cyclin E (LMW-E), exhibited higher rates of progression (13). The protein expressions of ER, cyclin E, γH2AX, pY-STAT3, and Rb were examined in two breast cancer patient cohorts—29 with metastatic disease and no evidence of progression on therapy and 25 with metastatic disease that progressed on therapy. All patients were treated at MDACC with either first-line (+ letrozole) or second-line (+ fulvestrant)

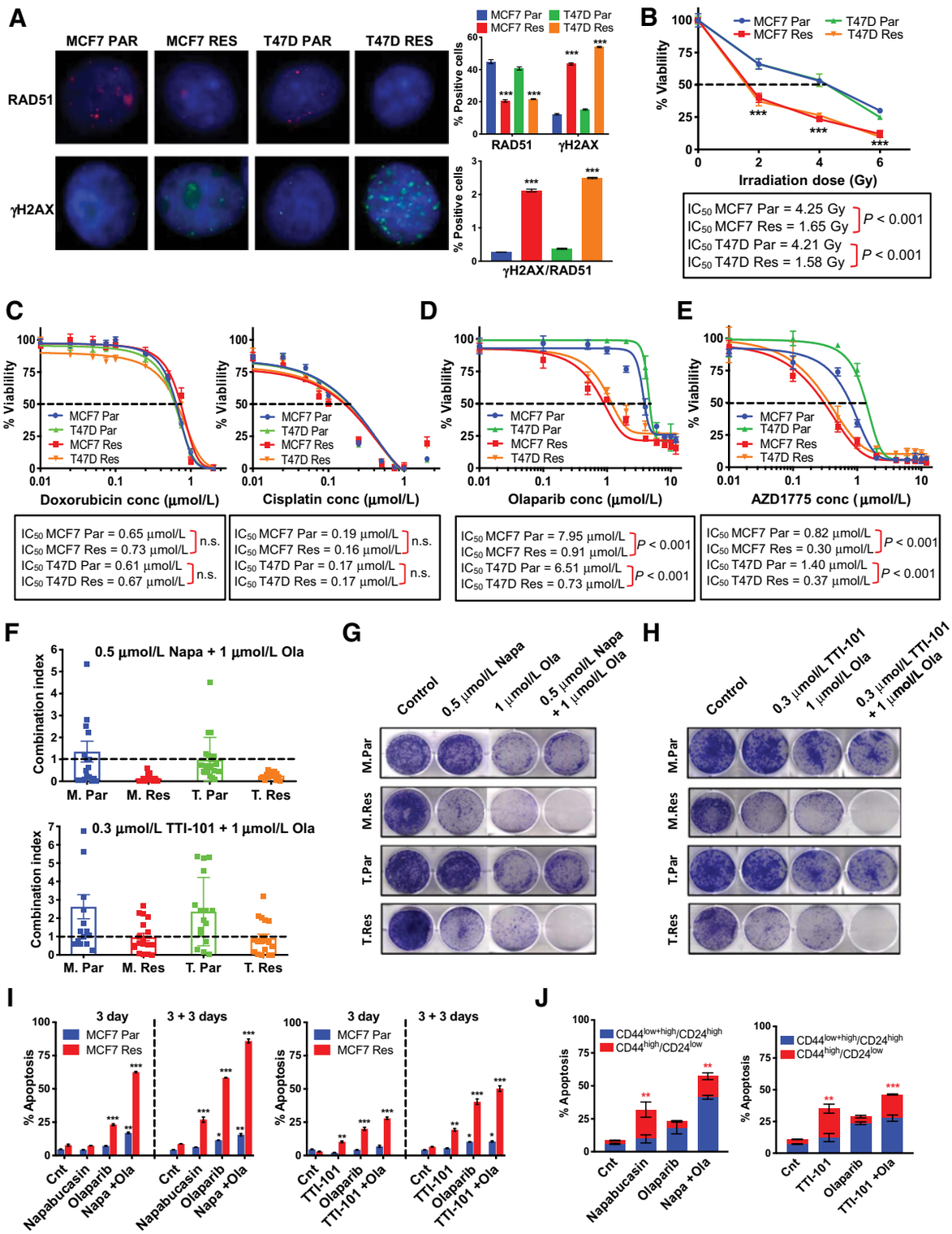

Figure 6.

DNA repair deficiency in the palbociclib-resistant cells sensitizes the cells to PARP and Wee1 inhibition, allowing for synergistic pathway inhibition in palbociclib-resistant cells with STAT3 inhibitors. **A,** Immunostaining of parental (Par) and resistant (Res) cells using antibodies against γH2AX and RAD51. γH2AX, RAD51, and DAPI are shown in green, red, and blue, respectively. Quantification of percent age of positive cells (bar graphs, top) shows resistant cells have decreased Rad51 foci and increased γH2AX foci. (*Continued on the following page.*)

therapy with palbociclib and assessment of key clinical and pathologic factors for the two cohorts (i.e., progressors and nonprogressors) revealed that there were no significant differences in any of the factors (Supplementary Tables S6 and S7). For the progressors we obtained matched biopsy specimens collected from each patient pretreatment and posttreatment (time of progression on therapy). Our IHC results showed that the percentage of ER-positive tumor cells was reduced in 12 of 25 (5/9 +fulvestrant; 7/16 +letrozole) palbociclib-resistant tumors ($P = 0.017$; Fig. 7A and B). In addition, we performed IHC for PR (Supplementary Fig. S7A and S7B), as PR is a target gene of ER and observed a positive linear correlation with ER posttreatment in the palbociclib-resistant tumors (Supplementary Fig. S7C). Cytoplasmic cyclin E (LMW-E), which in the pretreatment samples was expressed in 8 of 25 samples, increased in 15 of 25 samples in the postprogression cases ($P = 0.023$; Fig. 7C and D). Total DNA damage, as measured by γH2AX IHC, significantly increased in the postprogression tumor samples ($P = 0.032$; Fig. 7E and F). Furthermore, pY-STAT3 expression increased significantly in 14 of 25 patients in the postprogression samples ($P = 0.042$; Fig. 7G and H). We did not find a significant difference in pRb levels between the pre- and postprogression samples (Supplementary Fig. S7D). The alterations among ER, cytoplasmic cyclin E, γH2AX, and pY-STAT3 were heterogeneous across patients who progressed (Supplementary Table S8) but, there were no differences between the expression of these proteins between the nonprogressors and the preprogression samples (data not shown) suggesting that the changes in these four biomarkers observed in the postprogression samples is likely due to palbociclib-mediated mechanisms of resistance.

Discussion

CDK4/6 inhibitors in combination with endocrine therapy are currently considered standard of care for patients with advanced ER-positive breast cancer. Because many patients will develop resistance to CDK4/6 inhibitor therapy, understanding the mechanisms of acquired resistance to this class of agents is a critical unmet need. The results from our study have identified two clinically relevant, divergent, and druggable pathways (DNA repair and STAT3) that can be targeted in combination to effectively combat drug resistance. We also found that the same pathways that were deregulated in palbociclib-resistant cells were also altered in tumor samples obtained from patients who progressed while on palbociclib and endocrine therapy, providing the rationale for future biomarker driven clinical trials with therapies targeting these nonoverlapping pathways.

Although there is precedent for the development of therapies after progression on CDK4/6 inhibitors, as well as combination therapies with CDK4/6 inhibitors either first-line or second-line (2, 51), lack of biomarker driven clinical trials has curtailed efforts to identify the patients that are best suited for each of these trials. Some of the ongoing clinical trials are with different PI3K/mTOR inhibitors because activation of PI3K or mTOR has been associated with relapse (51), which we have also observed in our model of palbociclib resistance. These trials have shown improved progression-free survival with endocrine therapy combined with a PI3K or mTOR inhibitor with high clinical benefit in patients with *PIK3CA* mutations (52, 53). Results are still pending for a trial with the mTOR inhibitor everolimus, following CDK4/6 progression [TRINITI-1 trial (54); NCT02732119], but based on our data, Rb status may play an important role in response to mTOR inhibitors and could be used as a biomarker to screen patients who will benefit from this therapy.

An unexpected finding from our studies was the downregulation of the ER protein in both the preclinical palbociclib-resistant cell lines (Figs. 1 and 4), as well as tumor samples from patients who progressed on palbociclib with aromatase inhibitor therapy (Fig. 7). This finding is in accordance with known mechanisms of action of aromatase inhibitors through reducing estradiol levels and signaling through ER, with little or no inhibitory effect on ER levels; unlike fulvestrant, a selective ER antagonist, which reduces tumor ER protein levels (55, 56). In addition, a study investigating the mechanisms of resistance to abemaciclib showed that ER protein is downregulated in cells and in 3 of 7 patients examined, however, the type of endocrine therapy was not mentioned (5). The downregulation of ER in our resistant cell lines was also associated with downregulation of other hormone receptors, PR, AR, and GR and these cells were also less sensitive to RU486 (an inhibitor of PR/GR; Fig. 1F; Supplementary Fig. S1F and S1L). However, when the levels of FOXA1, a coactivator for ER signaling, was downregulated in the palbociclib-resistant cells, whereas ER mRNA levels were further reduced (Supplementary Fig. S1H and S1I), the downstream ER signaling pathways remained unabated (Supplementary Fig. S1J), suggesting alternate mechanisms for palbociclib-mediated ER downregulation.

We propose that the mechanism of ER downregulation is posttranslational through induction of IL6 (Fig. 3), which can also degrade ER protein (29). Furthermore, ER negatively regulates IL6 gene expression (28, 57); however, IL6 signaling may also negatively regulate ER, but the mechanism by which this occurs is not well studied. A recent study by Sansone and colleagues revealed that recombinant IL6 treatment in ER-positive breast cancer cells led to a reduction in ER protein (29), possibly through an ubiquitin–proteasome pathway (58). Finally, given

(*Continued.*) The ratio of γH2AX/RAD51-positive cells (bar graphs, bottom) is significantly increased in the resistant cells. **B,** Resistant (Res) cells are sensitive to ionizing radiation. Par, parental. **C,** Dose–response curves to doxorubicin and cisplatin in resistant (Res) and parental (Par) cells. conc, concentration. **D,** Dose–response curves show that resistant (Res) cells are sensitive to treatment with olaparib (PARP inhibitor). conc, concentration; Par, parental. **E,** Dose–response curves to AZD1775 (Wee1 inhibitor). conc, concentration; Par, parental; Res, resistant. **F,** Combination of napabucasin (Napa) and olaparib (Ola) or TTI-101 and Ola are synergistic in the resistant (Res) cell lines as shown by the plotted CI calculated by CalcuSyn. Par, parental. **G,** Clonogenic assay showing the combination effect of 1 μmol/L olaparib (Ola) and 0.5 μmol/L napabucasin (Napa) for 3 days and 9 days recovery. Par, parental; Res, resistant. **H,** Clonogenic assay showing the combination effect of 1 μmol/L olaparib (Ola) and 0.3 μmol/L TTI-101 for 3 days and 9 days recovery. Par, parental; Res, resistant. **I,** Apoptosis analysis by flow cytometry using Annexin V shows increased apoptosis in the MCF-7–resistant (Res) cells treated with the combination of olaparib (Ola) and napabucasin (Napa) or Ola and TTI-101 after 3 days of treatment and after 3 days recovery (3 + 3). Cnt, control; Par, parental. **J,** Flow cytometry analysis using Annexin V, CD44, and CD24 markers identifying the population of apoptotic cells that are B-CSC-L (red: $CD44^{high}/CD24^{low}$) or non-B-CSC-L (blue: $CD44^{low+high}/CD24^{high}$) after 3 days of treatment with olaparib (Ola), napabucasin (Napa), and TTI-101. Cnt, control; Par, parental; Res, resistant.

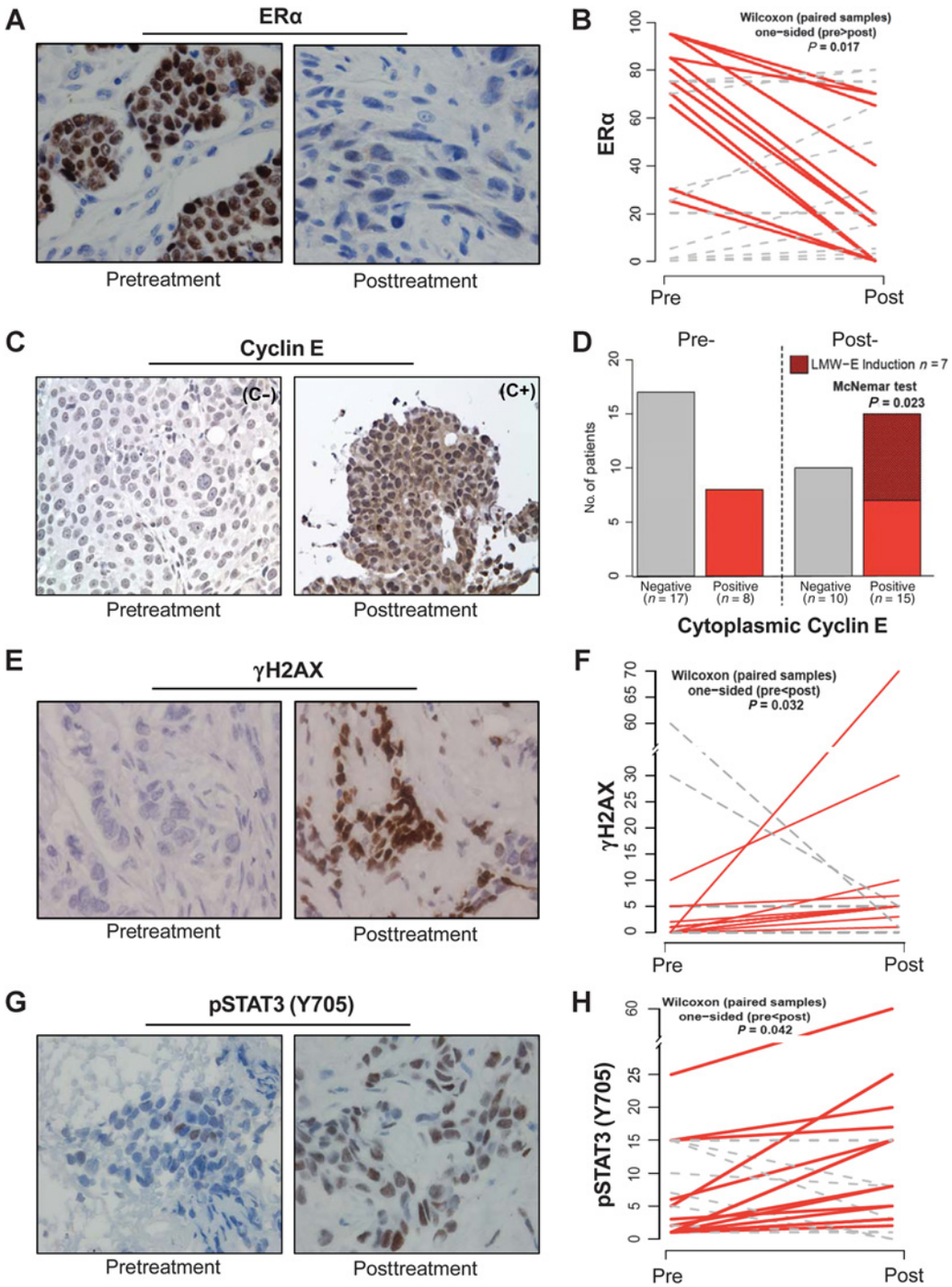

Figure 7.

Analysis of pre/post-palbociclib treatment tumor samples from patients with ER-positive metastatic breast cancer identifies potential biomarkers of acquired resistance. **A,** Representative IHC staining for ERα levels pre- and post-palbociclib treatment. **B,** Quantification of the 25 matched pre/post samples show an overall reduction in ER levels (red line) posttreatment even although some have no change or an increase in ERα (gray dashed line). **C,** Representative IHC for cyclin E showing negative or positive cytoplasmic (C− or C+) staining of cyclin E pre- and posttreatment. **D,** Quantification of cytoplasmic cyclin E shows that pretreatment for 8 of 25 tumors were positive for cytoplasmic cyclin E (LMW-E) and maintained positivity posttreatment (red bars). Of the 17 of 25 patients whose tumors were negative for LMW-E pretreatment, 10 remained negative posttreatment (gray bars), while 7 became positive (red-hashed bar) increasing the LMW-E positive samples from 8 of 25 (pre-progression) to 15 of 25 (post-progression). **E,** Representative IHC for γH2AX pre- and posttreatment. **F,** Quantification of γH2AX shows induction posttreatment (red lines) is significant ($P = 0.032$). **G,** Representative IHC for pY-STAT3 (Y705) pre- and posttreatment. **H,** Quantification of pY-STAT3 shows significant ($P = 0.042$) enrichment in posttreatment samples (red line).

the importance of IL6 signaling in driving STAT3 activation, ER has also been identified as a target gene of STAT3 by microarray and ChIP analyses (59), suggesting STAT3 may also regulate ER transcription.

In addition to its proposed roles in degradation of ER, IL6/STAT3 pathway is also associated with different features of oncogenesis, including metastasis, higher stages of disease progression and decreased survival (60). In breast cancer, IL6 is tumor promoting by itself and leads to resistance to doxorubicin (61) and activation of IL6/gp130/JAK2 pathway and increased autocrine signaling leading to STAT3 activation (62). We also showed that treatment of parental, palbociclib-sensitive cells with recombinant IL6 and its receptor, leads to downregulation of ER, increased levels of pY-STAT3, resistance to palbociclib, resistance to endocrine therapy, and increased sensitivity to STAT3 inhibitors (Fig. 4). These data suggest that treating a CDK4/6 inhibitor naïve cell line with IL6 generates a CDK4/6 inhibitor–resistant phenotype. Thus, induction of IL6 in the tumor may be a key mechanism of both endocrine and CDK4/6 inhibitor resistance. We also propose that because IL6 is induced in tumor cells it can give rise to increased IL6 locally within the tumor microenvironment, as well as systemically. Thus, measuring IL6 in the blood of patients undergoing CDK4/6 inhibitor based therapy may serve as a means to identify those patients who are likely to become resistant to these agents.

Functionally, we showed that palbociclib-resistant cells exhibit IL6/STAT3-mediated upregulation of EMT and B-CSC-L pathways, as well as downregulation of the DNA repair pathway (Figs. 3–6). The IL6/STAT3 and DNA repair pathways are divergent, hence inhibiting them in combination is unlikely to result in mechanisms of overlapping resistance. For example, we found that inhibition of STAT3 reduced the B-CSC-L population, whereas inhibition of DNA repair induced apoptosis in the non-B-CSC-L population. Thus, targeting these pathways in combination using STAT3 and PARP inhibitors proved highly effective in activating the apoptosis pathways resulting in cell killing of the palbociclib-resistant cells (Fig. 6).

Finally, we examined whether the same pathways that were altered in palbociclib-resistant cells were also altered in 25 matched pre- and posttreatment tumor samples obtained from patients who progressed while on palbociclib-containing therapies. Our results revealed that: (i) ER and PR are downregulated in these tumors, (ii) cytoplasmic cyclin E and γH2AX are increased, indicating accumulation of replicative stress and DNA damage (48, 49), and (iii) levels of pY-STAT3 are increased in the palbociclib progressors (Fig. 7). These results suggest that evaluation of ER, PR, cyclin E, γH2AX, and pY-STAT3 in biopsy samples from patients who develop resistance to CDK4/6 inhibitor–based therapies may aid in developing potential biomarker-based clinical trials with combination therapies targeting DNA damage and STAT3. Because of the limited patient cohort, the mechanism may be specific to this cohort, however, brief analysis of our larger patient cohort of 583 patients (Supplementary Fig. S7E and S7F and data not shown) is suggestive that the patient samples examined are a good representation of the whole cohort.

Disclosure of Potential Conflicts of Interest

N.K. Ibrahim is a consultant/advisory board member for Ipsen and Immunomedics. D.J. Tweardy receives compensation as a member of Tvardi Therapeutics' board of directors and scientific advisory board, and also holds equity in the company. K.K. Hunt reports receiving commercial research grants from Endomagnetics and Lumicell, and is a consultant/advisory board member for Armada Health and Merck & Co. D. Tripathy is a consultant/advisory board member for Pfizer and Novartis. No potential conflicts of interest were disclosed by the other authors.

Authors' Contributions

Conception and design: N.M. Kettner, S. Vijayaraghavan, J.P.W. Carey, N.K. Ibrahim, S.S. Watowich, A. Sahin, D.J. Tweardy, K.K. Hunt, D. Tripathy, K. Keyomarsi

Development of methodology: N.M. Kettner, S. Vijayaraghavan, B. Liu, J.P.W. Carey, D.J. Tweardy, K.K. Hunt, D. Tripathy, K. Keyomarsi

Acquisition of data (provided animals, acquired and managed patients, provided facilities, etc.): N.M. Kettner, S. Vijayaraghavan, M.G. Durak, M. Kohansal, J.P.W. Carey, X. Chen, T.K. Eckols, A.S. Raghavendra, N.K. Ibrahim, A. Sahin, D. Tripathy, K. Keyomarsi

Analysis and interpretation of data (e.g., statistical analysis, biostatistics, computational analysis): N.M. Kettner, S. Vijayaraghavan, M.J. Ha, B. Liu, X. Rao, J. Wang, M. Yi, A.S. Raghavendra, S.S. Watowich, D.J. Tweardy, K.K. Hunt, D. Tripathy, K. Keyomarsi

Writing, review, and/or revision of the manuscript: N.M. Kettner, S. Vijayaraghavan, M.G. Durak, X. Rao, M. Yi, N.K. Ibrahim, M.S. Karuturi, S.S. Watowich, A. Sahin, D.J. Tweardy, K.K. Hunt, D. Tripathy, K. Keyomarsi

Administrative, technical, or material support (i.e., reporting or organizing data, constructing databases): N.M. Kettner, S. Vijayaraghavan, T. Bui, T.K. Eckols, A. Sahin, D. Tripathy, K. Keyomarsi

Study supervision: K.K. Hunt, D. Tripathy, K. Keyomarsi

Acknowledgments

Research reported in this article was supported by the NCI of the NIH under award P30CA016672 to The University of Texas MD Anderson Cancer Center, the Department of Defense Breakthrough Post-Doctoral Fellowship BC170615 (to N.M. Kettner), R01 grant CA1522218, R01 grant CA223772, and Cancer Prevention and Research Institute of Texas (CPRIT) RP170079 grant (to K. Keyomarsi), CPRIT multi-investigator grant RP180712 (to K.K. Hunt and K. Keyomarsi), the Susan G. Komen for the Cure grant KG100521 (to K.K. Hunt), the Susan G. Komen post-doctoral fellowship grant PDF14302675 (to J.P.W. Carey), the CPRIT Research Training Program grant RP170067 (to S. Vijayaraghavan and N.M. Kettner), CPRIT grant DP150069 and V Foundation for Cancer Research Translational Research Award T2014-010 (to D.J. Tweardy), and NIH National Institute of Allergy and Infectious Diseases (NIAID) grant R01AI109294 (to S.S. Watowich).

The costs of publication of this article were defrayed in part by the payment of page charges. This article must therefore be hereby marked *advertisement* in accordance with 18 U.S.C. Section 1734 solely to indicate this fact.

Received October 5, 2018; revised February 3, 2019; accepted March 12, 2019; published first March 13, 2019.

References

1. Pan H, Gray R, Braybrooke J, Davies C, Taylor C, McGale P, et al. 20-year risks of breast-cancer recurrence after stopping endocrine therapy at 5 years. N Engl J Med 2017;377:1836–46.
2. Preusser M, De Mattos-Arruda L, Thill M, Criscitiello C, Bartsch R, Ruhstaller T, et al. CDK4/6 inhibitors in the treatment of patients with breast cancer: summary of a multidisciplinary round-table discussion. ESMO Open 2018;3:e000368.
3. Vijayaraghavan S, Moulder S, Keyomarsi K, Layman RM. Inhibiting CDK in cancer therapy: current evidence and future directions. Target Oncol 2018;13:21–38.
4. Herrera-Abreu MT, Palafox M, Asghar U, Rivas MA, Cutts RJ, Garcia-Murillas I, et al. Early adaptation and acquired resistance to CDK4/6 inhibition in estrogen receptor-positive breast cancer. Cancer Res 2016;76:2301–13.

5. Yang C, Li Z, Bhatt T, Dickler M, Giri D, Scaltriti M, et al. Acquired CDK6 amplification promotes breast cancer resistance to CDK4/6 inhibitors and loss of ER signaling and dependence. Oncogene 2017; 36:2255–64.
6. O'Leary B, Hrebien S, Morden JP, Beaney M, Fribbens C, Huang X, et al. Early circulating tumor DNA dynamics and clonal selection with palbociclib and fulvestrant for breast cancer. Nat Commun 2018;9:896.
7. de Leeuw R, McNair C, Schiewer MJ, Neupane NP, Brand LJ, Augello MA, et al. MAPK reliance via acquired CDK4/6 inhibitor resistance in cancer. Clin Cancer Res 2018;24:4201–14.
8. Jansen VM, Bhola NE, Bauer JA, Formisano L, Lee KM, Hutchinson KE, et al. Kinome-wide RNA interference screen reveals a role for PDK1 in acquired resistance to CDK4/6 inhibition in ER-positive breast cancer. Cancer Res 2017;77:2488–99.
9. Chen X, Low KH, Alexander A, Jiang Y, Karakas C, Hess KR, et al. Cyclin E overexpression sensitizes triple-negative breast cancer to Wee1 kinase inhibition. Clin Cancer Res 2018;24:6594–610.
10. Carey JPW, Karakas C, Bui T, Chen X, Vijayaraghavan S, Zhao Y, et al. Synthetic lethality of PARP inhibitors in combination with MYC blockade is independent of BRCA status in triple-negative breast cancer. Cancer Res 2018;78:742–57.
11. Duong MT, Akli S, Macalou S, Biernacka A, Debeb BG, Yi M, et al. Hbo1 is a cyclin E/CDK2 substrate that enriches breast cancer stem-like cells. Cancer Res 2013;73:5556–68.
12. Duong MT, Akli S, Wei C, Wingate HF, Liu W, Lu Y, et al. LMW-E/CDK2 deregulates acinar morphogenesis, induces tumorigenesis, and associates with the activated b-Raf-ERK1/2-mTOR pathway in breast cancer patients. PLoS Genet 2012;8:e1002538.
13. Vijayaraghavan S, Karakas C, Doostan I, Chen X, Bui T, Yi M, et al. CDK4/6 and autophagy inhibitors synergistically induce senescence in Rb positive cytoplasmic cyclin E negative cancers. Nat Commun 2017;8:15916.
14. Staff S, Tolonen T, Laasanen SL, Mecklin JP, Isola J, Maenpaa J. Quantitative analysis of gamma-H2AX and p53 nuclear expression levels in ovarian and fallopian tube epithelium from risk-reducing salpingo-oophorectomies in BRCA1 and BRCA2 mutation carriers. Int J Gynecol Pathol 2014;33: 309–16.
15. Love MI, Huber W, Anders S. Moderated estimation of fold change and dispersion for RNA-seq data with DESeq2. Genome Biol 2014;15:550.
16. Ross-Innes CS, Stark R, Teschendorff AE, Holmes KA, Ali HR, Dunning MJ, et al. Differential oestrogen receptor binding is associated with clinical outcome in breast cancer. Nature 2012;481:389–93.
17. Fu X, Jeselsohn R, Pereira R, Hollingsworth EF, Creighton CJ, Li F, et al. FOXA1 overexpression mediates endocrine resistance by altering the ER transcriptome and IL-8 expression in ER-positive breast cancer. Proc Natl Acad Sci U S A 2016;113:E6600–E9.
18. Carroll JS, Liu XS, Brodsky AS, Li W, Meyer CA, Szary AJ, et al. Chromosome-wide mapping of estrogen receptor binding reveals long-range regulation requiring the forkhead protein FoxA1. Cell 2005;122:33–43.
19. Pan D, Kocherginsky M, Conzen SD. Activation of the glucocorticoid receptor is associated with poor prognosis in estrogen receptor-negative breast cancer. Cancer Res 2011;71:6360–70.
20. Beischlag TV, Perdew GH. ER alpha-AHR-ARNT protein-protein interactions mediate estradiol-dependent transrepression of dioxin-inducible gene transcription. J Biol Chem 2005;280:21607–11.
21. Zhang J, Xu K, Liu P, Geng Y, Wang B, Gan W, et al. Inhibition of Rb phosphorylation leads to mTORC2-mediated activation of Akt. Mol Cell 2016;62:929–42.
22. Al-Hajj M, Wicha MS, Benito-Hernandez A, Morrison SJ, Clarke MF. Prospective identification of tumorigenic breast cancer cells. Proc Natl Acad Sci U S A 2003;100:3983–8.
23. Ginestier C, Hur MH, Charafe-Jauffret E, Monville F, Dutcher J, Brown M, et al. ALDH1 is a marker of normal and malignant human mammary stem cells and a predictor of poor clinical outcome. Cell Stem Cell 2007;1: 555–67.
24. Rota LM, Lazzarino DA, Ziegler AN, LeRoith D, Wood TL. Determining mammosphere-forming potential: application of the limiting dilution analysis. J Mammary Gland Biol Neoplasia 2012;17:119–23.
25. Roussos ET, Wang Y, Wyckoff JB, Sellers RS, Wang W, Li J, et al. Mena deficiency delays tumor progression and decreases metastasis in polyoma middle-T transgenic mouse mammary tumors. Breast Cancer Res 2010;12: R101.
26. Rohan TE, Xue X, Lin HM, D'Alfonso TM, Ginter PS, Oktay MH, et al. Tumor microenvironment of metastasis and risk of distant metastasis of breast cancer. J Natl Cancer Inst 2014;106:dju136.
27. Karagiannis GS, Pastoriza JM, Wang Y, Harney AS, Entenberg D, Pignatelli J, et al. Neoadjuvant chemotherapy induces breast cancer metastasis through a TMEM-mediated mechanism. Sci Transl Med 2017;9:.
28. Stein B, Yang MX. Repression of the interleukin-6 promoter by estrogen receptor is mediated by NF-kappa B and C/EBP beta. Mol Cell Biol 1995; 15:4971–9.
29. Sansone P, Ceccarelli C, Berishaj M, Chang Q, Rajasekhar VK, Perna F, et al. Self-renewal of CD133(hi) cells by IL6/Notch3 signalling regulates endocrine resistance in metastatic breast cancer. Nat Commun 2016;7:10442.
30. Haricharan S, Dong J, Hein S, Reddy JP, Du Z, Toneff M, et al. Mechanism and preclinical prevention of increased breast cancer risk caused by pregnancy. Elife 2013;2:e00996.
31. Johnson DE, O'Keefe RA, Grandis JR. Targeting the IL-6/JAK/STAT3 signalling axis in cancer. Nat Rev Clin Oncol 2018;15:234–48.
32. O'Shea JJ, Gadina M, Schreiber RD. Cytokine signaling in 2002: new surprises in the Jak/Stat pathway. Cell 2002;109:S121–31.
33. Schust J, Sperl B, Hollis A, Mayer TU, Berg T. Stattic: a small-molecule inhibitor of STAT3 activation and dimerization. Chem Biol 2006;13: 1235–42.
34. Redell MS, Ruiz MJ, Alonzo TA, Gerbing RB, Tweardy DJ. Stat3 signaling in acute myeloid leukemia: ligand-dependent and -independent activation and induction of apoptosis by a novel small-molecule Stat3 inhibitor. Blood 2011;117:5701–9.
35. Marcucci F, Rumio C, Lefoulon F. Anti-cancer stem-like cell compounds in clinical development - an overview and critical appraisal. Front Oncol 2016;6:115.
36. Zhang Y, Jin Z, Zhou H, Ou X, Xu Y, Li H, et al. Suppression of prostate cancer progression by cancer cell stemness inhibitor napabucasin. Cancer Med 2016;5:1251–8.
37. Marotta LL, Almendro V, Marusyk A, Shipitsin M, Schemme J, Walker SR, et al. The JAK2/STAT3 signaling pathway is required for growth of $CD44^{+}CD24^{-}$ stem cell-like breast cancer cells in human tumors. J Clin Invest 2011;121:2723–35.
38. Vriend LE, De Witt Hamer PC, Van Noorden CJ, Wurdinger T. WEE1 inhibition and genomic instability in cancer. Biochim Biophys Acta 2013; 1836:227–35.
39. Chou TC. Drug combination studies and their synergy quantification using the Chou-Talalay method. Cancer Res 2010;70:440–6.
40. Bijnsdorp IV, Giovannetti E, Peters GJ. Analysis of drug interactions. Methods Mol Biol 2011;731:421–34.
41. Konecny GE, Winterhoff B, Kolarova T, Qi J, Manivong K, Dering J, et al. Expression of p16 and retinoblastoma determines response to CDK4/6 inhibition in ovarian cancer. Clin Cancer Res 2011;17:1591–602.
42. Wiedemeyer WR, Dunn IF, Quayle SN, Zhang J, Chheda MG, Dunn GP, et al. Pattern of retinoblastoma pathway inactivation dictates response to CDK4/6 inhibition in GBM. Proc Natl Acad Sci U S A 2010;107: 11501–6.
43. Cen L, Carlson BL, Schroeder MA, Ostrem JL, Kitange GJ, Mladek AC, et al. p16-Cdk4-Rb axis controls sensitivity to a cyclin-dependent kinase inhibitor PD0332991 in glioblastoma xenograft cells. Neuro Oncol 2012;14: 870–81.
44. Finn RS, Crown JP, Lang I, Boer K, Bondarenko IM, Kulyk SO, et al. The cyclin-dependent kinase 4/6 inhibitor palbociclib in combination with letrozole versus letrozole alone as first-line treatment of oestrogen receptor-positive, HER2-negative, advanced breast cancer (PALOMA-1/TRIO-18): a randomised phase 2 study. Lancet Oncol 2015;16:25–35.
45. Clark AS, Karasic TB, DeMichele A, Vaughn DJ, O'Hara M, Perini R, et al. Palbociclib (PD0332991)-a selective and potent cyclin-dependent kinase inhibitor: a review of pharmacodynamics and clinical development. JAMA Oncol 2016;2:253–60.
46. Turner NC, Jiang Y, O'Leary B, Hrebien S, Cristofanilli M, Andre F, et al. Efficacy of palbociclib plus fulvestrant (P+F) in patients (pts) with metastatic breast cancer (MBC) and *ESR1* mutations (mus) in circulating tumor DNA (ctDNA). J Clin Oncol 34:15s, 2016 (suppl; abstr 512).
47. Cristofanilli M, Turner NC, Bondarenko I, Ro J, Im SA, Masuda N, et al. Fulvestrant plus palbociclib versus fulvestrant plus placebo for treatment of hormone-receptor-positive, HER2-negative metastatic breast cancer that progressed on previous endocrine therapy (PALOMA-3): final analysis of

the multicentre, double-blind, phase 3 randomised controlled trial. Lancet Oncol 2016;17:425–39.
48. Teixeira LK, Reed SI. Cyclin E deregulation and genomic instability. Adv Exp Med Biol 2017;1042:527–47.
49. Macheret M, Halazonetis TD. Intragenic origins due to short G1 phases underlie oncogene-induced DNA replication stress. Nature 2018;555: 112–6.
50. Caruso JA, Duong MT, Carey JPW, Hunt KK, Keyomarsi K. Low-molecular-weight cyclin E in human cancer: cellular consequences and opportunities for targeted therapies. Cancer Res 2018;78:5481–91.
51. Liu P, Cheng H, Roberts TM, Zhao JJ. Targeting the phosphoinositide 3-kinase pathway in cancer. Nat Rev Drug Discov 2009;8:627–44.
52. Mayer IA, Abramson VG, Formisano L, Balko JM, Estrada MV, Sanders ME, et al. A phase Ib study of alpelisib (BYL719), a PI3Kα-specific inhibitor, with letrozole in ER+/HER2- metastatic breast cancer. Clin Cancer Res 2017;23:26–34.
53. Hortobagyi GN. Everolimus plus exemestane for the treatment of advanced breast cancer: a review of subanalyses from BOLERO-2. Neoplasia 2015;17: 279–88.
54. Hurvitz S, Yardley D, Zelnak A, DeMichele A, Tan-Chiu E, Ma CX, et al. Ribociclib in combination with everolimus and exemestane in men and postmenopausal women with HR+/HER2− advanced breast cancer following progression on a CDK4/6 inhibitor: safety, tolerability, and pharmacokinetic results from phase 1 of TRINITI-1 study. [abstract]. In: Proceedings of the American Association for Cancer Research Annual Meeting 2017; 2017 Apr 1–5; Washington, DC. Philadelphia (PA): AACR; Cancer Res 2017;77(13 Suppl):Abstract nr CT110.
55. Robertson JF, Dixon JM, Sibbering DM, Jahan A, Ellis IO, Channon E, et al. A randomized trial to assess the biological activity of short-term (pre-surgical) fulvestrant 500 mg plus anastrozole versus fulvestrant 500 mg alone or anastrozole alone on primary breast cancer. Breast Cancer Res 2013;15:R18.
56. Arnedos M, Drury S, Afentakis M, A'Hern R, Hills M, Salter J, et al. Biomarker changes associated with the development of resistance to aromatase inhibitors (AIs) in estrogen receptor-positive breast cancer. Ann Oncol 2014;25:605–10.
57. Ray A, Prefontaine KE, Ray P. Down-modulation of interleukin-6 gene expression by 17 beta-estradiol in the absence of high affinity DNA binding by the estrogen receptor. J Biol Chem 1994;269:12940–6.
58. Tecalco-Cruz AC, Ramirez-Jarquin JO. Mechanisms that increase stability of estrogen receptor alpha in breast cancer. Clin Breast Cancer 2017;17: 1–10.
59. Snyder M, Huang XY, Zhang JJ. Identification of novel direct Stat3 target genes for control of growth and differentiation. J Biol Chem 2008;283: 3791–8.
60. Knupfer H, Preiss R. Lack of knowledge: breast cancer and the soluble interleukin-6 receptor. Breast Care 2010;5:177–80.
61. Conze D, Weiss L, Regen PS, Bhushan A, Weaver D, Johnson P, et al. Autocrine production of interleukin 6 causes multidrug resistance in breast cancer cells. Cancer Res 2001;61:8851–8.
62. Berishaj M, Gao SP, Ahmed S, Leslie K, Al-Ahmadie H, Gerald WL, et al. Stat3 is tyrosine-phosphorylated through the interleukin-6/glycoprotein 130/Janus kinase pathway in breast cancer. Breast Cancer Res 2007; 9:R32.